

One-Loop Self Energy and Renormalization of the Speed of Light for some Anisotropic Improved Quark Actions

Stefan Groote

Newman Laboratory, Cornell University, Ithaca, NY 14853, USA

and

Institut für Physik der Johannes-Gutenberg-Universität,

Staudingerweg 7, D-55099 Mainz, Germany

Junko Shigemitsu

Physics Department, The Ohio State University, Columbus, OH 43210, USA

Abstract

One-loop corrections to the fermion rest mass M_1 , wave function renormalization Z_2 and speed of light renormalization C_0 are presented for lattice actions that combine improved glue with clover or D234 quark actions and keep the temporal and spatial lattice spacings, a_t and a_s , distinct. We explore a range of values for the anisotropy parameter $\chi \equiv a_s/a_t$ and treat both massive and massless fermions.

PACS number(s): 11.10.Gh, 11.15.Ha, 12.38.Bx, 12.38.Gc

I. INTRODUCTION

Examples of successful employment of anisotropic lattices in lattice QCD simulations have been increasing lately. They include extensive studies of the glueball spectrum [1], investigations of heavy hybrid states [2,3] and calculations of quarkonium fine structure [4]. In most cases one is dealing with large states requiring large spatial volumes and also signals that can only be extracted from high statistics data. Working with highly improved actions on coarse lattices helps with the large volume and statistics problems, however, a coarse temporal lattice spacing means that correlation functions fall off very rapidly. This last problem can be circumvented by going to an anisotropic lattice which allows for a much finer temporal grid. The correlation functions can be sampled much more frequently in a given physical time region where the signal is still good.

Another potential use of anisotropic lattices would be in simulations of matrix elements in hadronic states with large momenta. These typically occur in semileptonic decays of heavy hadrons. Once one goes beyond spectrum calculations to matrix elements, one is faced with the matching problem between operators in the coarse highly improved lattice theory and continuum QCD. In this article we take a first step in accumulating necessary renormalization factors based on perturbation theory. We carry out the one-loop self energy calculation in several anisotropic improved quark actions. This gives us renormalization of the rest mass M_1 , the wave function renormalization Z_2 and the “speed of light” renormalization, C_0 , a quantity which will be defined more precisely in the following sections. We treat both massive and massless quarks. Perturbation theory can be used not only in operator matchings, but also to fix parameters in the lattice actions. C_0 is an example of one such parameter.

In the next section we introduce the gauge and quark actions considered in this article. Section 3 describes the general formalism that we employ for the self energy calculation with massive fermions. We follow closely the work of the Fermilab group [5] which we could straightforwardly extend to anisotropic actions. Section 4 discusses specific one-loop contributions for mass, wavefunction and speed of light renormalizations. Our results are tabulated in section 5 for various choices of actions, fermion masses and degree of anisotropy. Some calculational details are left for appendices, where we describe Feynman rules and IR subtractions in our calculations.

II. GAUGE AND QUARK ACTIONS

We work with two classes of gauge actions denoted \mathcal{S}_G^I and \mathcal{S}_G^{II} [6,7], with

$$\begin{aligned} \mathcal{S}_G^I = & -\beta \sum_{x,s>s'} \frac{1}{\chi} \left\{ c_0^G \frac{P_{ss'}}{u_s^4} + c_1^G \frac{R_{ss'}}{u_s^6} + c_1^G \frac{R_{s's}}{u_s^6} \right\} \\ & -\beta \sum_{x,s} \chi \left\{ c_0^G \frac{P_{st}}{u_s^2 u_t^2} + c_1^G \frac{R_{st}}{u_s^4 u_t^2} + c_1^G \frac{R_{ts}}{u_t^4 u_s^2} \right\} \end{aligned} \quad (1)$$

and

$$\begin{aligned} \mathcal{S}_G^{II} = & -\beta \sum_{x,s>s'} \frac{1}{\chi} \left\{ \frac{5}{3} \frac{P_{ss'}}{u_s^4} - \frac{1}{12} \frac{R_{ss'}}{u_s^6} - \frac{1}{12} \frac{R_{s's}}{u_s^6} \right\} \\ & -\beta \sum_{x,s} \chi \left\{ \frac{4}{3} \frac{P_{st}}{u_s^2 u_t^2} - \frac{1}{12} \frac{R_{st}}{u_s^4 u_t^2} \right\}. \end{aligned} \quad (2)$$

The x sum is over lattice sites and the variable s runs over spatial directions. $\beta \equiv 2N_c/g^2$, χ is the anisotropy parameter

$$\chi = a_s/a_t \quad (3)$$

and

$$P_{\mu\nu} = \frac{1}{N_c} \text{Real} \left(\text{Tr} \{ U_\mu(x) U_\nu(x + a_\mu) U_\mu^\dagger(x + a_\nu) U_\nu^\dagger(x) \} \right), \quad (4)$$

$$R_{\mu\nu} = \frac{1}{N_c} \text{Real} \left(\text{Tr} \{ U_\mu(x) U_\mu(x + a_\mu) U_\nu(x + 2a_\mu) U_\mu^\dagger(x + a_\mu + a_\nu) U_\mu^\dagger(x + a_\nu) U_\nu^\dagger(x) \} \right). \quad (5)$$

u_s and u_t are the tadpole improvement parameters u_0 for spatial and temporal link variables respectively [8].

The parameters c_0^G and c_1^G in action \mathcal{S}_G^I are constrained to satisfy $c_0^G + 8c_1^G = 1$. The Symanzik improved gauge action, in which $O(a^2)$ errors are removed, corresponds to $c_0^G = 5/3$ and $c_1^G = -1/12$ [9], whereas $c_0^G = 3.648$ and $c_1^G = -0.331$, for $\chi = 1$, leads to one of the RG improved Iwasaki actions [10]. In \mathcal{S}_G^{II} parameters have been fixed to the Symanzik values. We will be working mainly with Symanzik improved actions and present RG improved results only for a few cases. We note that the action \mathcal{S}_G^{II} is intrinsically asymmetric even for the isotropic limit $\chi = 1$.

The most highly improved quark action that we have analysed is the $D234$ action [6].

$$\begin{aligned} \mathcal{S}_{D234}^I = & a_s^3 a_t \sum_x \bar{\Psi}_c \left\{ \gamma_t \frac{1}{a_t} (\nabla_t - \frac{1}{6} C_{3t} \nabla_t^{(3)}) + \frac{C_0}{a_s} \vec{\gamma} \cdot (\vec{\nabla} - \frac{1}{6} C_3 \vec{\nabla}^{(3)}) + m_0 \right. \\ & \left. - \frac{r a_s}{2} \left[\frac{1}{a_t^2} (\nabla_t^{(2)} - \frac{1}{12} C_{4t} \nabla_t^{(4)}) + \frac{1}{a_s^2} \sum_j (\nabla_j^{(2)} - \frac{1}{12} C_4 \nabla_j^{(4)}) \right] \right. \\ & \left. - r a_s \frac{C_F}{4} \frac{i \sigma_{\mu\nu} \tilde{F}^{\mu\nu}}{a_\mu a_\nu} \right\} \Psi_c \end{aligned} \quad (6)$$

$$\begin{aligned} = & \sum_x \bar{\Psi}_L \left\{ \gamma_t (\nabla_t - \frac{1}{6} C_{3t} \nabla_t^{(3)}) + \frac{C_0}{\chi} \vec{\gamma} \cdot (\vec{\nabla} - \frac{1}{6} C_3 \vec{\nabla}^{(3)}) + a_t m_0 \right. \\ & \left. - \frac{r}{2} \left[\chi (\nabla_t^{(2)} - \frac{1}{12} C_{4t} \nabla_t^{(4)}) + \frac{1}{\chi} \sum_j (\nabla_j^{(2)} - \frac{1}{12} C_4 \nabla_j^{(4)}) \right] \right. \\ & \left. - r \frac{C_F}{4} i \sigma_{\mu\nu} \tilde{F}^{\mu\nu} \frac{a_s a_t}{a_\mu a_\nu} \right\} \Psi_L. \end{aligned} \quad (7)$$

The quark fields Ψ_c and the dimensionless lattice fields Ψ_L are related through

$$\Psi_L = a_s^{3/2} \Psi_c. \quad (8)$$

The dimensionless derivatives $\nabla^{(n)}$ and field strength tensors $\tilde{F}^{\mu\nu}$ are tadpole improved [8] and defined in the Appendix. We use the convention $\sigma_{\mu\nu} = \frac{1}{2}[\gamma_\mu, \gamma_\nu]$ and set $r = 1$ in all our calculations. At tree-level the coefficients $C_0, C_3, C_{3t}, C_4, C_{4t}$ and C_F are equal to one. The quark action is then tree-level accurate through $O(a_s^3)$ and $O(a_t^3)$. C_0 is what we call the “speed of light”. This parameter is adjusted, in general either perturbatively or nonperturbatively, to ensure correct dispersion relations for particles. In anticipation of working on anisotropic lattices with a_t much finer than a_s , one can drop the higher order improvement terms in the temporal derivatives by setting $C_{3t} = C_{4t} = 0$, without loosing accuracy. We call this action \mathcal{S}_{D234}^{II} .

$$\begin{aligned} \mathcal{S}_{D234}^{II} = \sum_x \bar{\Psi}_L \left\{ \gamma_t \nabla_t + \frac{C_0}{\chi} \vec{\gamma} \cdot (\vec{\nabla} - \frac{1}{6} C_3 \vec{\nabla}^{(3)}) + a_t m_0 \right. \\ \left. - \frac{r}{2} \left[\chi \nabla_t^{(2)} + \frac{1}{\chi} \sum_j (\nabla_j^{(2)} - \frac{1}{12} C_4 \nabla_j^{(4)}) \right] \right. \\ \left. - r \frac{C_F}{4} i \sigma_{\mu\nu} \tilde{F}^{\mu\nu} \frac{a_s a_t}{a_\mu a_\nu} \right\} \Psi_L \end{aligned} \quad (9)$$

The familiar $O(a)$ accurate clover quark [11] action corresponds to setting $C_3 = C_4 = 0$ in the above and using a less improved field strength tensor $F^{\mu\nu}$ (also defined in the Appendix) rather than $\tilde{F}^{\mu\nu}$.

$$\begin{aligned} \mathcal{S}_{clover} = \sum_x \bar{\Psi}_L \left\{ \gamma_t \nabla_t + \frac{C_0}{\chi} \vec{\gamma} \cdot \vec{\nabla} + a_t m_0 \right. \\ \left. - \frac{r}{2} \left[\chi \nabla_t^{(2)} + \frac{1}{\chi} \sum_j \nabla_j^{(2)} \right] - r \frac{C_F}{4} i \sigma_{\mu\nu} F^{\mu\nu} \frac{a_s a_t}{a_\mu a_\nu} \right\} \Psi_L \end{aligned} \quad (10)$$

We have carried out one-loop self energy calculations for several combinations of the above gauge and quark actions, for both massless and massive quarks. We list the specific actions considered in Table I. For actions \mathcal{S}^A and $\mathcal{S}^{A'}$ massless results have already appeared in [12]. We agree with their results and we include these cases here for completeness. With action \mathcal{S}^C we treat only the massless case, since our formalism for massive quarks, following [5], requires that the only time derivatives be in the ∇_t and $\nabla_t^{(2)}$ terms. Both \mathcal{S}_{D234}^{II} and \mathcal{S}_{clover} satisfy this condition, but \mathcal{S}_{D234}^I does not.

III. GENERAL FORMALISM FOR SELF ENERGY CALCULATIONS

In this section we summarize the formalism for self energy calculations, along the lines of reference [5]. Perturbative calculations for massive Wilson quarks are also described in reference [13]. We concentrate on the massive case, since massless lattice perturbation theory has been in the literature for decades.

For massive fermions we use either \mathcal{S}_{D234}^{II} or \mathcal{S}_{clover} . The fermion self energy $\Sigma(p)$ is defined in terms of the momentum space propagators $\overline{G}(p)$ and $\overline{G}_0(p)$ for the full and free theories respectively, as

$$\overline{G}^{-1}(p) = \overline{G}_0^{-1}(p) - \Sigma(p). \quad (11)$$

Carrying out the Fourier transform in p_0 one defines

$$\begin{aligned} G(t, \vec{p}) &= \int_{-\pi/a_t}^{\pi/a_t} \frac{dp_0}{2\pi} e^{ip_0 t} \overline{G}(p_0, \vec{p}) \\ &\equiv \mathcal{Z}_2(\vec{p}) e^{-E(\vec{p})t} \Gamma_{proj} + \dots \end{aligned} \quad (12)$$

Γ_{proj} is a projection operator in Dirac space. The ellipses refer to lattice artifacts and additional multi-particle states that could be created by the lattice fermion field operator Ψ beyond the single quark state. The rest mass, M_1 , is defined as

$$M_1 = E(\vec{p} = \vec{0}). \quad (13)$$

We do not consider the kinetic mass, M_2 [5] in this article. We will renormalize at the point $(p_0, \vec{p}) = (iM_1, \vec{0})$ and define the wave function renormalization constant

$$Z_2 = \mathcal{Z}_2(\vec{p} = \vec{0}). \quad (14)$$

For a zero spatial momentum quark propagating forward in time one expects ($t > 0$)

$$\begin{aligned} G(t, 0) &= \int_{-\pi/a_t}^{\pi/a_t} \frac{dp_0}{2\pi} e^{ip_0 t} \overline{G}(p_0, 0) \\ &\equiv Z_2 e^{-M_1 t} \frac{1 + \gamma_0}{2} + \dots \end{aligned} \quad (15)$$

Our goal in this section is to relate Z_2 and M_1 to parameters in the action and to $\Sigma(p)$. In order to orient ourselves, however, it is useful to first consider the free case with $\Sigma(p) = 0$.

A. Free Anisotropic Propagator

The free propagator $\overline{G}_0(p_0, \vec{p} = 0)$ for both actions \mathcal{S}_{D234}^{II} and \mathcal{S}_{clover} becomes (for $r = 1$)

$$\begin{aligned} \frac{1}{a_t} \overline{G}_0(p_0, \vec{p} = 0) &= \frac{1}{i\gamma_0 \sin(a_t p_0) + a_t m_0 + \chi - \chi \cos(a_t p_0)} \\ &= \frac{-i\gamma_0 \sin(a_t p_0) + a_t m_0 + \chi - \chi \cos(a_t p_0)}{(\sin(a_t p_0))^2 + [(a_t m_0 + \chi) - \chi \cos(a_t p_0)]^2}. \end{aligned} \quad (16)$$

In terms of the variable

$$z \equiv e^{ia_t p_0} = e^{-a_t E} \quad (17)$$

($p_0 = iE$), one finds two zeros of the denominator corresponding to positive energy solutions.

$$z_1 = \frac{(a_t m_0 + \chi) - \sqrt{(a_t m_0 + \chi)^2 + 1 - \chi^2}}{\chi - 1} \quad (18)$$

and

$$\tilde{z}_1 = \frac{(a_t m_0 + \chi) - \sqrt{(a_t m_0 + \chi)^2 + 1 - \chi^2}}{\chi + 1}. \quad (19)$$

The other two zeros, z_2 and \tilde{z}_2 correspond to negative energy solutions, $z_2 = 1/z_1$ and $\tilde{z}_2 = 1/\tilde{z}_1$. The integral over p_0 in (15) can be done as a contour integral around the unit circle in the variable z . One picks up contributions from both positive energy solutions (for $t > 0$).

$$\text{pole at } z_1 : \quad \frac{(1 + \gamma_0)}{2} \frac{e^{-M_1^{(0)} t}}{\sqrt{(a_t m_0 + \chi)^2 + 1 - \chi^2}}, \quad (20)$$

$$\text{pole at } \tilde{z}_1 : \quad \frac{(1 - \gamma_0)}{2} \frac{e^{-\tilde{M}_1^{(0)} t}}{\sqrt{(a_t m_0 + \chi)^2 + 1 - \chi^2}}, \quad (21)$$

with

$$a_t M_1^{(0)} = -\ln(z_1), \quad a_t \tilde{M}_1^{(0)} = -\ln(\tilde{z}_1). \quad (22)$$

Clearly, z_1 is the physical positive energy solution. The second solution \tilde{z}_1 is a lattice artifact, similar to the time doubler for $r \neq 1$ in isotropic actions. The solution \tilde{z}_1 disappears in the isotropic limit, $\chi \rightarrow 1$, where $a_t \tilde{M}_1^{(0)} \rightarrow \infty$. In the same limit the physical solution z_1 goes over into the well known result

$$z_1 \rightarrow \frac{1}{1 + a_t m_0}. \quad (23)$$

The gap between $\tilde{M}_1^{(0)}$ and $M_1^{(0)}$, measured in units of $1/a_s$ is

$$a_s(\tilde{M}_1^{(0)} - M_1^{(0)}) = \chi \ln \frac{(\chi + 1)}{(\chi - 1)}, \quad (24)$$

independent of m_0 . This becomes ∞ at $\chi = 1$ and approaches 2 as $\chi \rightarrow \infty$. The size of this gap, $a_s \delta E \geq 2$, is hence equal to or larger than the amount by which conventional spatial doublers are raised through the Wilson mechanism. We will henceforth ignore \tilde{z}_1 and concentrate on the physical pole at $z = z_1$. Comparing (20) with (15) one sees that there is nontrivial mass dependent wave function renormalization even at tree-level with

$$Z_2^{(0)} = \frac{1}{\sqrt{(a_t m_0 + \chi)^2 + 1 - \chi^2}} = \frac{1}{\chi \sinh(a_t M_1^{(0)}) + \cosh(a_t M_1^{(0)})}. \quad (25)$$

This has been pointed out several times in the literature [14,15].

A useful way to rewrite (18) is

$$a_t m_0 + \chi = \chi \cosh(a_t M_1^{(0)}) + \sinh(a_t M_1^{(0)}). \quad (26)$$

B. Mass Renormalization

In the interacting case one has a nontrivial $\Sigma(p)$ which we write as

$$a_t \Sigma(p) = i\gamma_0 B_0(p, m_0) \sin(a_t p_0) + i \frac{1}{\chi} \sum_j [\gamma_j B_j(p, m_0) \sin(a_s p_j)] + C(p, m_0). \quad (27)$$

The $\vec{p} = 0$ propagator becomes

$$\frac{1}{a_t} \overline{G}(p_0, \vec{p} = 0) = \frac{-i\gamma_0(1 - B_0) \sin(a_t p_0) + a_t m_0 + \chi - C - \chi \cos(a_t p_0)}{(1 - B_0)^2 [\sin(a_t p_0)]^2 + [(a_t m_0 + \chi) - C - \chi \cos(a_t p_0)]^2}, \quad (28)$$

where, $B_0 = B_0(p_0, m_0)$ and $C = C(p_0, m_0)$ are evaluated at $\vec{p} = 0$. If $p_0 = iE$ is the location of a pole in (28), the following implicit equation must be satisfied.

$$(1 - B_0(iE, m_0)) \sinh(a_t E) = \pm [(a_t m_0 + \chi) - C(iE, m_0) - \chi \cosh(a_t E)]. \quad (29)$$

One can check that the “+” sign leads to the pole $M_1^{(0)}$ in the free limit. Hence, the implicit equation for M_1 is given by

$$\chi \cosh(a_t M_1) + \sinh(a_t M_1) = a_t m_0 + \chi + B_0(iM_1, m_0) \sinh(a_t M_1) - C(iM_1, m_0). \quad (30)$$

In a perturbative calculation of M_1 one expands

$$M_1 = M_1^{(0)} + \alpha_s M_1^{(1)} + O(\alpha_s^2). \quad (31)$$

B_0 and C in (30) start out $O(\alpha_s)$, so through one-loop their argument can be replaced by the tree-level $M_1^{(0)}$. Expanding the LHS also through $O(\alpha_s)$ and taking (26) into account, one finds

$$\begin{aligned} \alpha_s a_t M_1^{(1)} &= \frac{B_0(iM_1^{(0)}, m_0) \sinh(a_t M_1^{(0)}) - C(iM_1^{(0)}, m_0)}{\chi \sinh(a_t M_1^{(0)}) + \cosh(a_t M_1^{(0)})} \\ &= - Z_2^{(0)} \text{tr} \left\{ \frac{(\gamma_0 + 1)}{4} a_t \Sigma(p_0 = iM_1^{(0)}, \vec{p} = 0) \right\}, \end{aligned} \quad (32)$$

where the trace is taken over Dirac space. We note that in the $M_1^{(0)} = 0, m_0 = 0$ limit, the γ_0 part of the trace $\text{tr}\{(\gamma_0 + 1)\Sigma\}$ does not contribute and one has

$$\alpha_s a_t M_1^{(1)}(0) = - \text{tr} \{a_t \Sigma(0)\} / 4 = -C(0, 0). \quad (33)$$

In order to have massless quarks remain massless under renormalization, one needs to carry out additive mass renormalization and $M_1^{(1)}$ in (32) requires a subtraction. This subtraction must be done without jeopardizing the pole condition (30). There is a standard way to accomplish this. Let m_c be the value of the bare quark mass parameter m_0 for which the physical quark rest mass vanishes ($M_1 = 0$). Eqn.(30) then tells us that m_c is implicitly defined through

$$a_t m_c - C(0, m_c) = 0. \quad (34)$$

In equations such as (28) or (30) one always has the combination $a_t m_0 - C$. Using (34) one can add and subtract $a_t m_c$ so that

$$a_t m_0 - C \rightarrow a_t(m_0 - m_c) - (C - C(0, m_c)) = a_t m - \tilde{C}. \quad (35)$$

Previous derivations go through with m_0 replaced by

$$m \equiv m_0 - m_c \quad (36)$$

and $C(iM_1, m_0)$ by

$$\tilde{C}(iM_1, m_0) = C(iM_1, m_0) - C(0, m_c). \quad (37)$$

In most lattice simulations, m_c and hence also m are determined nonperturbatively from the simulations themselves. For \tilde{C} , however, one still often uses the one-loop result

$$\tilde{C}(iM_1^{(0)}, m_0) = \tilde{C}(iM_1^{(0)}, m) = C(iM_1^{(0)}, m) - C(0, 0). \quad (38)$$

$M_1^{(0)}$ is now given in terms of m rather than m_0 . We will be presenting our results as functions of $a_s M_1^{(0)}$, with the understanding that the shift $m_0 \rightarrow m_0 - m_c$ has been carried out and that, for instance, $M_1^{(0)}$ is given by

$$a_t m + \chi = \chi \cosh(a_t M_1^{(0)}) + \sinh(a_t M_1^{(0)}) \quad (39)$$

rather than by (26). In (32) one needs to replace C by \tilde{C} . Our final formula for the one-loop mass correction, measured in units of $1/a_s$ then becomes

$$\begin{aligned} \alpha_s a_s M_{1,sub}^{(1)} &= \chi \frac{B_0(iM_1^{(0)}, m) \sinh(a_t M_1^{(0)}) - \tilde{C}(iM_1^{(0)}, m)}{\chi \sinh(a_t M_1^{(0)}) + \cosh(a_t M_1^{(0)})} \\ &= -Z_2^{(0)} \operatorname{tr} \left\{ \frac{(\gamma_0 + 1)}{4} \left[a_s \Sigma(p_0 = iM_1^{(0)}, \vec{p} = 0, m) - a_s \Sigma(0, \vec{0}, 0) \right] \right\}. \end{aligned} \quad (40)$$

This expression vanishes automatically for $M_1^{(0)} = m = 0$. We prefer to measure dimensionful quantities in terms of $1/a_s$ rather than $1/a_t$. When exploring $\chi \geq 1$ it makes more sense to fix a_s and let a_t be arbitrarily fine, rather than to fix a_t and let a_s become arbitrarily coarse. In the isotropic limit (40) agrees with formulas in the literature [5,13].

C. Wave Function Renormalization

In order to extract a general formula for the wave function renormalization Z_2 we need to find the residue of $\overline{G}(p_0, \vec{p} = 0)$ at the pole $p_0 = iM_1$. In terms of the variable z the Fourier transform in (15) has the form

$$\oint_{|z|=1} \frac{dz}{(2\pi i)z} (z)^{t/a_t} \frac{g(z)}{f(z)}, \quad (41)$$

where the integral is taken over the unit circle. To find the residue we expand the denominator around $z_1 = e^{-a_t M_1}$

$$f(z) = (z - z_1) \left(\frac{df}{dz} \right)_{z=z_1} + \dots \quad (42)$$

The contribution from the physical pole to $G(t, 0)$ is then

$$e^{-M_1 t} \left(\frac{g(z)}{z f'(z)} \right)_{z=z_1} . \quad (43)$$

One finds for the numerator

$$g(z = z_1) = (\gamma_0 + 1)(1 - B_0(iM_1, m)) \sinh(a_t M_1) \quad (44)$$

and for the denominator

$$2(1 - B_0(iM_1, m)) \sinh(a_t M_1) \times \left\{ \chi \sinh(a_t M_1) + \cosh(a_t M_1) + \left(i \frac{d}{d(a_t p_0)} [i B_0(p_0, m) \sin(a_t p_0) + C(p_0, m)] \right)_{p_0=iM_1} \right\} \quad (45)$$

using

$$\left(z \frac{df}{dz} \right)_{z=z_1} = -i \left(\frac{df}{d(a_t p_0)} \right)_{p_0=iM_1} . \quad (46)$$

One can now read off Z_2 and after recognizing the last term in (45) as derivatives acting on different parts of $a_t \Sigma(p_0, \vec{p} = 0, m)$, one obtains

$$Z_2^{-1} = \chi \sinh(a_t M_1) + \cosh(a_t M_1) + i \operatorname{tr} \left(\frac{(\gamma_0 + 1)}{4} \frac{d}{dp_0} \Sigma(p_0, \vec{p} = 0, m) \right)_{p_0=iM_1} . \quad (47)$$

The one-loop approximation to Z_2 is obtained by expanding M_1 once again in α_s .

$$\begin{aligned} Z_2^{-1} &= \chi \sinh(a_t M_1^{(0)}) + \cosh(a_t M_1^{(0)}) + \alpha_s a_t M_{1,sub}^{(1)} (\chi \cosh(a_t M_1^{(0)}) + \sinh(a_t M_1^{(0)})) \\ &\quad + i \operatorname{tr} \left(\frac{(\gamma_0 + 1)}{4} \frac{d}{dp_0} \Sigma(p_0, \vec{p} = 0, m) \right)_{p_0=iM_1^{(0)}} \\ &= Z_2^{(0)-1} \left[1 + \frac{\alpha_s}{\chi} a_s M_{1,sub}^{(1)} (\chi \cosh(a_t M_1^{(0)}) + \sinh(a_t M_1^{(0)})) Z_2^{(0)} \right. \\ &\quad \left. + i \operatorname{tr} \left(\frac{(\gamma_0 + 1)}{4} \frac{d}{dp_0} \Sigma(p_0, \vec{p} = 0, m) \right)_{p_0=iM_1^{(0)}} Z_2^{(0)} \right] + O(\alpha_s^2). \end{aligned} \quad (48)$$

In the last expression we have found it convenient to factor out the tree-level $Z_2^{(0)-1}$. Equations (47) and (48) go over into the formulas of [5] in the isotropic limit.

D. Speed of Light Renormalization

In order to discuss renormalization of the speed of light one needs to look at the inverse momentum space propagator at small but nonzero spatial momentum.

$$\begin{aligned}
a_t \bar{G}^{-1}(p) &= a_t \bar{G}_0^{-1}(p) - a_t \Sigma(p) \\
&= i \gamma_0 (1 - B_0) \sin(a_t p_0) + i \frac{1}{\chi} \sum_j [\gamma_j (C_0 K_j - B_j) \sin(a_s p_j)] \\
&\quad + a_t m + \chi - \chi \cos(a_t p_0) - C,
\end{aligned} \tag{49}$$

with $K_j = 1$ for \mathcal{S}_{clover} and $K_j = (4 - \cos(a_s p_j))/3$ for \mathcal{S}_{D234}^{II} . One can rewrite $\bar{G}^{-1}(p)$ as

$$\begin{aligned}
a_t \bar{G}^{-1}(p) &= (1 - B_0) \left\{ i \gamma_0 \sin(a_t p_0) + i \frac{1}{\chi} \sum_j \left[\gamma_j \frac{(C_0 K_j - B_j)}{(1 - B_0)} \sin(a_s p_j) \right] \right\} \\
&\quad + a_t m + \chi - \chi \cos(a_t p_0) - C.
\end{aligned} \tag{50}$$

C_0 is adjusted so that for small $a_s p_j$ the relative coefficient of the $\gamma_0 \sin(a_t p_0)$ and the $\gamma_j a_s p_j / \chi$ terms remains equal to unity. $(C_0 K_j - B_j) \sin(a_s p_j) = (C_0 - B_j) a_s p_j$ for all quark actions in this limit (of course, $K_j \sin(a_s p_j)$ is a better approximation to the continuum $a_s p_j$ in the $D234$ action than in the clover action), and one has

$$C_0 = 1 + B_j(C_0) - B_0(C_0) \approx 1 + B_j(C_0 = 1) - B_0(C_0 = 1) + O(\alpha_s^2). \tag{51}$$

Just as with Z_2 we will define the speed of light renormalization at the zero spatial momentum mass shell point $p = (iM_1, \vec{0})$. From (27) the two terms B_j and B_0 needed for C_0 at one-loop can be extracted through

$$B_j = -i \frac{\chi}{4} \text{tr} \left(\gamma_j \frac{\partial}{\partial(a_s p_j)} a_t \Sigma(p) \right)_{p=(iM_1^{(0)}, \vec{0})}, \tag{52}$$

$$B_0 = -\frac{1}{4} \frac{\text{tr}(\gamma_0 a_t \Sigma(iM_1^{(0)}, \vec{0}))}{\sinh(a_t M_1^{(0)})} \quad m > 0 \tag{53}$$

or

$$= -\frac{i}{4} \text{tr} \left(\gamma_0 \frac{\partial}{\partial p_0} \Sigma(p) \right)_{p=(0, \vec{0})} \quad m = 0. \tag{54}$$

We note that in the massive case there is nontrivial renormalization of C_0 even in the isotropic limit $\chi = 1$, due to our noncovariant mass shell condition, $p = (iM_1, \vec{0})$. Nevertheless, we believe the above definition of the renormalization of the speed of light is a sensible and physical one.

IV. ONE-LOOP CONTRIBUTIONS TO $\Sigma(P)$

In the previous section one-loop corrections for M_1 , Z_2 and C_0 were determined in terms of traces over $\Sigma(p)$ or over derivatives acting on $\Sigma(p)$. In this section we describe the lattice

perturbation theory diagrams that contribute to $\Sigma(p)$ at one loop. For all quark actions considered one can write

$$\Sigma(p) = \Sigma^{reg}(p) + \Sigma^{tad}(p) + \Sigma^{t.i.}(p). \quad (55)$$

Σ^{reg} is the regular ‘‘rainbow’’ diagram, the only diagram that exists in a continuum self energy calculation. Σ^{tad} denotes contributions from the lattice artifact tadpole diagram and $\Sigma^{t.i.}$ comes from perturbatively expanding the u_s ’s and u_t ’s entering definitions of tadpole improved derivatives (see Appendix). The main idea behind tadpole-improved perturbation theory [8] is to have $\Sigma^{t.i.}$ cancel the bulk of Σ^{tad} . We find in many instances, especially with \mathcal{S}_{clover} , that cancellation is complete if one uses the Landau link definition for u_s and u_t and works in Landau gauge.

A. $\Sigma^{reg}(p)$

In terms of the gauge propagator $D_{\mu\nu}$, quark propagator \bar{G}_0 and the vertex functions V_μ , one can write $a_t \Sigma^{reg}(p)$ as the following loop integral over the dimensionless momentum variables $-\pi \leq k_\mu \leq \pi$.

$$\begin{aligned} & a_t \Sigma^{reg}(p) \\ &= g^2 \frac{4}{3} \sum_{\mu,\nu} \int \frac{d^4 k}{(2\pi)^4} \left\{ V_\mu(ap, ap - k) \frac{\bar{G}_0(ap - k)}{a_t} V_\nu(ap - k, ap) \right\} D_{\mu\nu}(k, \alpha_g) \\ &= g^2 \frac{4}{3} \sum_{\mu,\nu} \int \frac{d^4 k}{(2\pi)^4} \left\{ V_\mu(ap, ap - k) [-i\gamma \cdot K \sin + \Omega]_{(ap-k)} V_\nu(ap - k, ap) \right\} \frac{D_{\mu\nu}(k, \alpha_g)}{(K^2 \sin^2 + \Omega^2)_{(ap-k)}} \end{aligned} \quad (56)$$

where, ap stands for $(a_t p_0, a_s \vec{p})$ and $K \sin$ for $K_0 \sin((ap - k)_0)$ or for $K_j \sin((ap - k)_j)/\chi$. $K_\mu(k)$, $\Omega(k)$, $V_\mu(k', k)$ and $D_{\mu\nu}(k, \alpha_g)$ are detailed in the Appendix. The argument α_g in the gauge propagator comes from the gauge fixing term, with $\alpha_g = 1$ and $\alpha_g = 0$ corresponding to Feynman and Landau gauges respectively. Our codes have been written for general α_g and we have used gauge invariance of M_1 and C_0 as one check on our results.

Equation (56) has the familiar form for a self energy integral. The only subtlety is to verify that one is indeed calculating Σ^{reg} measured in units of $1/a_t$, given the conventions in our Feynman rules. As explained in the Appendix, we choose to work with a dimensionless momentum space gauge propagator $D_{\mu\nu}$. It comes from the Fourier transform of the dimensionless correlator $\langle (a_\mu A_\mu) (a_\nu A_\nu) \rangle$. The relation between $D_{\mu\nu}$ and a more conventional propagator of dimension $1/(\text{energy})^2$, denoted $\tilde{D}_{\mu\nu}$, is

$$D_{\mu\nu} = \frac{a_\mu a_\nu}{a_s^3 a_t} \tilde{D}_{\mu\nu}. \quad (57)$$

Our vertex functions, V_μ , are also subtly different from those in isotropic lattice perturbation theory. They keep track of the $1/a_\mu$ in the derivatives, i.e. of whether one has a $1/a_s$ or $1/a_t$ there. If \tilde{V}_μ are vertex functions normalized such that $\tilde{V}_\mu \rightarrow -i\gamma_\mu$ for all μ in the continuum limit, then the relation to the V_μ of (56) is given by

$$V_\mu = \frac{a_t}{a_\mu} \tilde{V}_\mu. \quad (58)$$

Using (57) and (58) one can write

$$\begin{aligned} a_t \Sigma^{reg}(p) &= g^2 \frac{4}{3} \sum_{\mu, \nu} \int \frac{d^4 k}{(2\pi)^4} \left\{ \left(\frac{a_t}{a_\mu} \tilde{V}_\mu \right) \frac{\overline{G}_0}{a_t} \left(\frac{a_t}{a_\nu} \tilde{V}_\nu \right) \right\} \left(\frac{a_\mu a_\nu}{a_s^3 a_t} \tilde{D}_{\mu\nu} \right) \\ &= a_t g^2 \frac{4}{3} \sum_{\mu, \nu} \int \frac{d^4 k}{(2\pi)^4 a_s^3 a_t} \left\{ \tilde{V}_\mu \overline{G}_0 \tilde{V}_\nu \right\} \tilde{D}_{\mu\nu}. \end{aligned} \quad (59)$$

To evaluate (56) we made extensive use of the symbolic manipulation package Mathematica. The integrals themselves were done using the VEGAS program [16]. The various steps involving Mathematica were to 1. calculate the products $V_\mu[-i\gamma \cdot K \sin + \Omega]V_\nu$; 2. carry out the Dirac traces such as $tr\{(1 + \gamma_0)\Sigma\}$; 3. take derivatives with respect to external momenta; 4. put things on the mass shell $p = (iM_1, \vec{0})$; and 5. use trigonometric identities to re-express the full integrands in (56) in terms of powers of $\hat{k}_\mu \equiv 2 \sin(k_\mu/2)$. The last step facilitated speedy evaluation of the integrand by VEGAS.

Both M_1 and C_0 are physical quantities. In addition to being gauge invariant they are also IR finite. The wave function renormalization Z_2 , on the other hand, is gauge dependent and also generally logarithmically IR divergent. In any calculation of a physical quantity this IR divergence will eventually be cancelled by vertex corrections and/or matching to continuum operators. In this article we will isolate the gauge dependent IR divergence in Z_2 , verify that it is the same as in the corresponding continuum theory and present results for the remaining IR finite parts. The IR divergence is found in the contribution from Σ^{reg} to Z_2 . More specifically it resides in the following term in (48)

$$i \operatorname{tr} \left(\frac{(\gamma_0 + 1)}{4} \frac{d}{dp_0} \Sigma^{reg}(p_0, \vec{p} = 0, m) \right)_{p_0=iM_1^{(0)}} Z_2^{(0)}. \quad (60)$$

We adopt the method of reference [13] to subtract IR divergent contributions inside integrands and rewrite (60) as

$$\begin{aligned} \int_k \left\{ \sum_{\mu, \nu} i \operatorname{tr} \left(\frac{(\gamma_0 + 1)}{4} \frac{d}{dp_0} \left[V_\mu \frac{\overline{G}_0}{a_t} V_\nu \right]_{p_0=iM_1^{(0)}} D_{\mu\nu} Z_2^{(0)} \right) - \mathcal{F}_{sub}(k, m_{eff}, \Lambda, \lambda) \right\} \\ + F(m_{eff}, \Lambda, \lambda), \end{aligned} \quad (61)$$

with

$$F(m_{eff}, \Lambda, \lambda) = \int_k \mathcal{F}_{sub}(k, m_{eff}, \Lambda, \lambda) \quad (62)$$

and

$$\int_k \equiv g^2 \frac{4}{3} \int \frac{d^4 k}{(2\pi)^4}. \quad (63)$$

Explicit forms for $\mathcal{F}_{sub}(k, m_{eff}, \Lambda, \lambda)$ and $F(m_{eff}, \Lambda, \lambda)$ are given in the Appendix. λ is a gluon mass introduced to regulate IR divergences. \mathcal{F}_{sub} has been constructed to match the same IR divergence as the first term inside the integral in (61). As a result the integral becomes independent of λ . The other condition on \mathcal{F}_{sub} is that the integral (62) be easy to do analytically. The simplest approach is to use a continuum self energy expression for \mathcal{F}_{sub} with an appropriate choice for the mass parameter m_{eff} . The need to adjust m_{eff} to optimize matching of the IR behaviours in \mathcal{F}_{sub} and the lattice integrand, was emphasized in reference [13] and following that work we find

$$a_t m_{eff} = \sinh(a_t M_1^{(0)}) \frac{\cosh(a_t M_1^{(0)}) + \chi \sinh(a_t M_1^{(0)})}{1 + \chi \sinh(a_t M_1^{(0)})}. \quad (64)$$

The same \mathcal{F}_{sub} and m_{eff} work for both the clover and D234 quark actions since the IR structure of the two theories agree. Finally, $\Lambda \leq \pi$ in the above expressions is a cutoff imposed on \mathcal{F}_{sub} so that $\mathcal{F}_{sub} = 0$ for $k^2 > \Lambda^2$. The full expression (61) must be independent of Λ .

B. $\Sigma^{tad}(p)$

The second contribution to $\Sigma(p)$ is the tadpole contribution $\Sigma^{tad}(p)$ coming from the two-gluon emission vertices listed in the Appendix. For quark action \mathcal{S}_{D234}^{II} one has

$$\begin{aligned} a_t \Sigma^{tad}(p) &= \frac{1}{2} [i\gamma_0 \sin(a_t p_0) - \chi \cos(a_t p_0)] \int_k D_{00} \\ &+ \frac{1}{2\chi} \frac{1}{3} \sum_j \int_k D_{jj} \left\{ i\gamma_j \left[(3 + C_3) \sin(a_s p_j) - 2C_3 \sin(2a_s p_j) \cos\left(\frac{k_j}{2}\right) \right] \right. \\ &\left. - \left[(3 + C_4) \cos(a_s p_j) - C_4 \cos(2a_s p_j) \cos^2\left(\frac{k_j}{2}\right) \right] \right\}. \end{aligned} \quad (65)$$

$\Sigma^{tad}(p)$ in the case of \mathcal{S}_{clover} is obtained by setting $C_3 = C_4 = 0$ in the above expression. The appropriate traces and derivatives with respect to external momenta can be carried out immediately and one has

$$\begin{aligned} &-tr \left\{ \frac{(\gamma_0 + 1)}{4} a_t \Sigma^{tad} \right\}_{p=(iM_1^{(0)}, \vec{0})} \\ &= \begin{cases} \frac{1}{2} [\sinh(a_t M_1^{(0)}) + \chi \cosh(a_t M_1^{(0)})] \int_k D_{00} + \frac{1}{2\chi} \sum_j \int_k D_{jj} & \mathcal{S}_{clover} \\ \frac{1}{2} [\sinh(a_t M_1^{(0)}) + \chi \cosh(a_t M_1^{(0)})] \int_k D_{00} + \frac{1}{6\chi} \sum_j \int_k D_{jj} [4 - \cos^2(\frac{k_j}{2})] & \mathcal{S}_{D234}^{II} \end{cases} \end{aligned} \quad (66)$$

$$i \operatorname{tr} \left\{ \frac{(\gamma_0 + 1)}{4} \frac{d}{dp_0} \Sigma^{tad} \right\}_{p=(iM_1^{(0)}, \vec{0})} = -\frac{1}{2} [\cosh(a_t M_1^{(0)}) + \chi \sinh(a_t M_1^{(0)})] \int_k D_{00} \quad (67)$$

$\mathcal{S}_{clover} \text{ \& } \mathcal{S}_{D234}^{II}$

$$B_j^{tad} - B_0^{tad} = \begin{cases} \frac{1}{2} \int_k D_{jj} - \frac{1}{2} \int_k D_{00} & \mathcal{S}_{clover} \\ \frac{2}{3} \int_k D_{jj} \sin^2(\frac{k_j}{2}) - \frac{1}{2} \int_k D_{00} & \mathcal{S}_{D234}^I \end{cases} \quad (68)$$

where B_j^{tad} and B_0^{tad} are the contributions from the tadpole diagram to (52) and (53) or (54). All the integrals are IR finite and very easy to carry out numerically. Contributions from Σ^{tad} typically dominate over those from Σ^{reg} but the bulk if not all of it is cancelled by $\Sigma^{t.i.}$.

C. $\Sigma^{t.i.}(p)$

The lattice covariant derivatives in the quark actions are tadpole-improved. They are listed in the Appendix. In momentum space one has, for instance

$$\nabla_\mu \rightarrow i \sin(a_\mu p_\mu) / u_\mu \approx i \sin(a_\mu p_\mu) [1 + \alpha_s u_\mu^{(2)}] + O(\alpha_s^2), \quad (69)$$

where we have perturbatively expanded

$$u_\mu = 1 - \alpha_s u_\mu^{(2)} + O(\alpha_s^2). \quad (70)$$

Even in the absence of the regular and tadpole one-loop diagrams there are hence $O(\alpha_s)$ terms in the quark propagator. We denote the inverse quark propagator with the u_μ 's still in place as $\overline{G}_{0,u0}^{-1}(p)$, so that $\overline{G}_0^{-1}(p) \equiv \overline{G}_{0,u0=1}^{-1}(p)$. Through $O(\alpha_s)$ eqn.(11) can be written as

$$\overline{G}^{-1} = \overline{G}_{0,u0}^{-1} - \Sigma^{reg} - \Sigma^{tad} \equiv \overline{G}_0^{-1} - \Sigma^{reg} - \Sigma^{tad} - \Sigma^{t.i.} \quad (71)$$

or

$$\Sigma^{t.i.} = \overline{G}_{0,u0=1}^{-1} - \overline{G}_{0,u0}^{-1}. \quad (72)$$

From the difference in (72) one sees that one link hops bring in factors of $1 - 1/u_\mu \approx -\alpha_s u_\mu^{(2)}$ and two link hops factors of $1 - 1/u_\mu^2 \approx -2\alpha_s u_\mu^{(2)}$ etc. Using these rules one finds

$$\begin{aligned} a_t \Sigma^{t.i.}(p) &= \alpha_s u_t^{(2)} [-i\gamma_0 \sin(a_t p_0) + \chi \cos(a_t p_0)] + \\ &\quad \alpha_s u_s^{(2)} \frac{1}{3\chi} \sum_j \{ -i\gamma_j [(3 + C_3) \sin(a_s p_j) - C_3 \sin(2a_s p_j)] \\ &\quad + [(3 + C_4) \cos(a_s p_j) - \frac{C_4}{2} \cos(2a_s p_j)] \}. \end{aligned} \quad (73)$$

The relevant traces and derivatives become

$$\begin{aligned}
& -tr \left\{ \frac{(\gamma_0 + 1)}{4} a_t \Sigma^{t.i.} \right\}_{p=(iM_1^{(0)}, \vec{0})} \\
& = \begin{cases} -[\sinh(a_t M_1^{(0)}) + \chi \cosh(a_t M_1^{(0)})] \alpha_s u_t^{(2)} - \frac{3}{\chi} \alpha_s u_s^{(2)} & \mathcal{S}_{clover} \\ -[\sinh(a_t M_1^{(0)}) + \chi \cosh(a_t M_1^{(0)})] \alpha_s u_t^{(2)} - \frac{1}{\chi} \frac{7}{2} \alpha_s u_s^{(2)} & \mathcal{S}_{D234}^{II} \end{cases} \quad (74)
\end{aligned}$$

$$\begin{aligned}
i \, tr \left\{ \frac{(\gamma_0 + 1)}{4} \frac{d}{dp_0} \Sigma^{t.i.} \right\}_{p=(iM_1^{(0)}, \vec{0})} & = [\cosh(a_t M_1^{(0)}) + \chi \sinh(a_t M_1^{(0)})] \alpha_s u_t^{(2)} \quad (75) \\
& \mathcal{S}_{clover} \ \& \ \mathcal{S}_{D234}^{II}
\end{aligned}$$

$$B_j^{t.i.} - B_0^{t.i.} = \begin{cases} \alpha_s (u_t^{(2)} - u_s^{(2)}) & \mathcal{S}_{clover} \\ \alpha_s (u_t^{(2)} - \frac{2}{3} u_s^{(2)}) & \mathcal{S}_{D234}^{II} \end{cases} \quad (76)$$

The Landau mean link definition of u_μ is given by

$$u_\mu \equiv \langle \frac{1}{3} Tr U_\mu \rangle_{\alpha_g=0} \approx 1 - \alpha_s u_\mu^{(2)} = 1 - \frac{1}{2} \int_k D_{\mu\mu}(\alpha_g = 0). \quad (77)$$

If one evaluates Σ^{tad} in Landau gauge then (66) & (74), (67) & (75) and (68) & (76) cancel for \mathcal{S}_{clover} . (67) & (75) also cancel for \mathcal{S}_{D234}^{II} and for the other two traces cancellation is almost complete. The difference between contributions from Σ^{tad} and $\Sigma^{t.i.}$ would go away if one replaces $\cos^2(k/2)$ and $\sin^2(k/2)$ by their averages $1/2$. Hence, it is easy to see in this calculation how tadpole improving terms in the lattice action eliminates lattice artifact contributions in perturbation theory.

V. RESULTS

In this section we summarize results for the one-loop coefficients, $a_s M_{1,sub}^{(1)}$, $Z_2^{(1)}$ and $C_0^{(1)}$ for mass, wave function and speed of light renormalizations respectively. These follow from equations (40), (48) and (51) - (54) and each has, as explained in the previous section, contributions from regular, tadpole and t.i. diagrams. The numbers in our Tables are coefficients of α_s . The Landau mean link definition of u_μ is used throughout to implement tadpole improvement.

A. $a_s M_{1,sub}^{(1)}$

In Table II we present results for $a_s M_{1,sub}^{(1)}$ for action \mathcal{S}^A for several values of $a_s M_1^{(0)}$. We list separately contributions from Σ^{reg} , Σ^{tad} and $\Sigma^{t.i.}$. The fourth column gives the gauge invariant combination (reg + tad) and the sixth column gives $a_s M_{1,nosub}^{(1)} \equiv$ (reg + tad +

t.i.), the full tadpole improved one-loop correction before subtraction. Carrying out the subtraction according to (40), one obtains $a_s M_{1,sub}^{(1)}$ which is given in the last column

$$a_s M_{1,sub}^{(1)} = a_s M_{1,nosub}^{(1)} - \frac{a_s M_{1,nosub}^{(1)}(0)}{\chi \sinh(a_t M_1^{(0)}) + \cosh(a_t M_1^{(0)})}. \quad (78)$$

All our calculations have been carried out for two values of the gauge fixing parameter α_g , 1.0 and 0.0. Table II lists both sets of results and one sees that gauge invariant quantities are independent of α_g within numerical integration errors (which we take to be at the ± 0.003 to ± 0.006 level depending on the mass). Our results for $a_s M_1^{(0)} = 0$ agree with those from [12].

We plot $a_s M_{1,sub}^{(1)}$ versus $a_s M_1^{(0)}$ in Fig. 1. One sees that the mass dependence is smooth and that one reaches saturation rapidly already around $a_s M_1^{(0)} \sim 3.0 - 5.0$. We also compare with non-tadpole improved results for which the curve saturates around 1.827 rather than around 1.077. In considering the large mass limit it is useful to note that the factor $Z_2^{(0)} = 1/[\chi \sinh(a_t M_1^{(0)}) + \cosh(a_t M_1^{(0)})]$ appearing in (40) and (48) vanishes exponentially in this limit. The only terms that survive into the static limit are those where $Z_2^{(0)}$ is multiplied by an exponentially increasing function of $a_s M_1^{(0)}$. It is easy to see, for instance, that the subtraction term in (78) or the spatial tadpoles in (66) become irrelevant in the static limit. Furthermore $a_s M_{1,sub}^{(1)}$ becomes identical for \mathcal{S}_{Wilson} , \mathcal{S}_{clover} and \mathcal{S}_{D234}^{II} in this limit and the only difference between the current calculations and those of reference [17] resides in the glue action (we have verified that by switching to the unimproved Wilson glue action results of [17] are reproduced).

In Tables III, IV and V we summarize results for $a_s M_{1,sub}^{(1)}$ for the other actions listed in Table I. We also list the combination (reg + tad) for each case. If one chooses to implement tadpole improvement differently from what we have done here or decides not to tadpole improve, then $a_s M_{1,sub}^{(1)}$ can be calculated straightforwardly from (reg + tad) and the formulas presented in this paper. For action \mathcal{S}^C we list only massless results for reasons explained in section II. The dispersion relations of this and similar actions are discussed in reference [18]. Our choices for anisotropy values in Tables IV and V, were dictated in part with an eye towards practical numerical simulations. Values such as $\chi = 3.6$ and $\chi = 5.3$ were taken from recent work on nonperturbative determinations of the renormalized anisotropy in pure glue theory [19]. For one value $a_s M_1^{(0)} = 1$ we plot $a_s M_{1,sub}^{(1)}$ versus χ in Fig. 2 using the action \mathcal{S}^D . From Tables IV and V and from Fig. 2 one sees that the dependence of $a_s M_{1,sub}^{(1)}$ on χ is very mild. Effects of tadpole improvement are significant only for small values of χ . This is because due to cancellations in the subtraction of equation (78) only the temporal tadpole and the temporal Landau link term $u_t^{(2)}$ contribute to $a_s M_{1,sub}^{(1)}$ and both these become small as χ increases.

Finally we mention that the one-loop expression for the critical bare mass m_c is given by

$$a_t m_c = -\frac{\alpha_s}{\chi} a_s M_{1,nosub}^{(1)}(0) + O(\alpha_s^2). \quad (79)$$

B. $Z_2^{(1)}$

Starting with (48) we define

$$Z_2 = Z_2^{(0)} [1 + \alpha_s (Z_2^{(1)} + Z_2^{(1)IR}) + O(\alpha_s^2)] \quad (80)$$

with

$$Z_2^{(1)IR} = \begin{cases} \frac{1}{3\pi} [1 + (\alpha_g - 1)] \ln(\lambda^2) & m = 0 \\ \frac{1}{3\pi} [-2 + (\alpha_g - 1)] \ln(\lambda^2) & m > 0 \end{cases} \quad (81)$$

λ is the gluon mass in units of $1/a_s$. It is the coefficient of α_s after factoring out $Z_2^{(0)}$ that has the same IR $\ln(\lambda)$ and $\ln(am)$ structure as the continuum wave function renormalization constant. From (48) one also sees that there are two contributions to $Z_2^{(1)}$, one coming from the d/dp_0 derivative term and the second from the expansion of M_1 . Accordingly we write

$$Z_2^{(1)} = Z_{2,dp_0}^{(1)} + Z_{2,M_1}^{(1)}. \quad (82)$$

In the literature $Z_{2,M_1}^{(1)}$ is not always included as part of the definition of $Z_2^{(1)}$. $Z_{2,dp_0}^{(1)}$ alone with unimproved Wilson glue goes over in the large mass limit to the wave function renormalization of reference [17]. Including $Z_{2,M_1}^{(1)}$ leads to the static result of reference [20] which has been used in many subsequent static calculations, for instance in [21]. This latter static value also corresponds to the large mass limit of the one-loop Z_2 calculated in many versions of NRQCD actions [22].

Table VI presents results for $Z_{2,dp_0}^{(1)}$ and the full $Z_2^{(1)}$ for the action \mathcal{S}^A . Again we agree with reference [12] for $m = 0$. However, one notices that the massive data do not tend towards the massless result as $a_s M_1^{(0)}$ decreases. This is because our massive numbers include $\ln(am)$ contributions which will eventually diverge, whereas in the massless theory we have set the fermion mass identical to zero from the beginning. This leads to different IR structure for the two theories (see Appendix B for some further discussions). In a matching calculation one will be looking at differences between the lattice and continuum Z_2 . As long as IR divergences are handled in the same manner in the lattice and continuum evaluations, one should not run into any problems and the $m \rightarrow 0$ limit should be smooth. For instance, using dimensional regularization in the \overline{MS} scheme one finds in Feynman gauge the UV finite continuum results

$$Z_2^{(1)cont.} = \begin{cases} \frac{1}{3\pi} \left[\ln\left(\frac{\lambda^2}{\mu^2}\right) + \frac{1}{2} \right] & m = 0 \\ \frac{1}{3\pi} \left[\ln\left(\frac{m^2}{\mu^2}\right) + 2 \ln\left(\frac{m^2}{\lambda^2}\right) - 4 \right] & m > 0 \end{cases} \quad (83)$$

Taking the difference between continuum and lattice wave function renormalization constants, it makes sense to consider the following subtracted Z_2 factors.

$$Z_{2,diff}^{(1)} = Z_{2,dp_0}^{(1)} - \begin{cases} \frac{1}{3\pi} \frac{1}{2} & m = 0 \\ \frac{1}{3\pi} [3 \ln(a_s M_1^{(0)})^2 - 4] & m > 0 \end{cases} \quad (84)$$

Numbers for $Z_{2,diff}^{(1)}$ are given in Table VII and one sees that the $m \rightarrow 0$ behaviour is smooth.

In Tables VIII through XII we present $Z_{2,dp0}^{(1)}$ and $Z_2^{(1)}$ for other actions. One does not find any dramatic changes with differing actions and/or anisotropy. The IR subtractions of Appendix B worked well in all actions for $a_s M_1^{(0)} < \sim 5$. For larger masses VEGAS errors became large especially for $\chi = 1$. Hence, we only present results up to $a_s M_1^{(0)} = 5$. For $\chi > 1$ problems were less severe in general. In Tables VI - XII the numerical integration errors are at the ± 0.02 level for $a_s M_1^{(0)} = 5.0$ and $\chi < 3$, at the ± 0.006 level for $a_s M_1^{(0)} = 0.01, 0.05$ and 0.10 and at the ± 0.004 level for all other cases. A more sophisticated method for handling IR divergent integrals appears necessary if accurate results are required for larger masses. Many quantities, however, are close to saturation by the time one reaches $a_s M_1^{(0)} = 5$.

C. $C_0^{(1)}$

For the speed of light renormalization we present the most detailed results for action \mathcal{S}^B rather than for \mathcal{S}^A since the former, for $\chi > 1$, is genuinely anisotropic. In Table XIII we list separately *regular* and *tadpole* diagram contributions, their gauge invariant sum ($reg + tad \equiv C_0^{(1)}$ *no t.i.*) and the fully tadpole improved result ($C_0^{(1)}$ *with t.i.*), all for action \mathcal{S}^B and at fixed anisotropy $\chi = 4.0$. $C_0^{(1)}$ is independent of α_g within numerical integration errors which are the most severe when using (53) for nonzero but small masses. In Figure 3. we plot $C_0^{(1)}$ both with and without tadpole improvement versus $a_s M_1^{(0)}$. Table XIV summarizes results for several χ values with action \mathcal{S}^B and in Figure 4. we plot $C_0^{(1)}$ versus χ for fixed $a_s M_1^{(0)} = 1.0$. One sees that tadpole improvement has significant effect and causes $C_0^{(1)}$ to switch sign for $\chi > 1$. Among other things this allows for a smooth $\chi \rightarrow 1$ limit.

In Table XV we present results for actions \mathcal{S}^A and $\mathcal{S}^{A'}$. In these isotropic actions nontrivial C_0 comes about because our mass-shell condition $p = (iM_1, \vec{0})$ distinguishes between spatial and temporal directions once $M_1 > 0$. Table XVI summarizes results for action \mathcal{S}^D . Here tadpole improvement does not decrease the magnitude of the one-loop correction, however, for a wide range of mass values it is still true that $C_0^{(1)}$ switches sign for $\chi > 1$ and that the $\chi \rightarrow 1$ limit becomes smoother after tadpole improvement.

VI. SUMMARY

We have carried out one-loop perturbative renormalization of the fermion rest mass M_1 , wave function renormalization Z_2 and the speed of light C_0 for a range of highly improved actions on isotropic and anisotropic lattices. We find that the dependence of the one-loop coefficients on the anisotropy parameter $\chi = a_s/a_t$ and on the tree-level mass parameter $a_s M_1^{(0)}$ is mild, especially after tadpole improvement of the actions. Furthermore, none of the coefficients are particularly large. M_1 and C_0 exhibit smooth behaviour as one approaches the massless, large mass, $\chi \rightarrow 1$ and large χ limits. This also holds for Z_2 if more

physical combinations such as the difference between continuum and lattice wave function renormalizations are considered. The next stage in our program would be to extend the present calculations to vertex corrections and to matchings between continuum and lattice currents and other multi-fermion operators.

VII. ACKNOWLEDGMENTS

This research is supported by grants from the US Department of Energy, DE-FG02-91ER40690, and from the Graduiertenkolleg. The authors thank Peter Lepage for many useful conversations. S.G. gratefully acknowledges a grant given by the Max Kade Foundation. J.S. thanks Cornell University for its hospitality while the project was being initiated and the theoretical physics group at the University of Glasgow where part of the work was carried out. Support from a UK PPARC Visiting Fellowship PPA/V/S/1997/00666 is gratefully acknowledged.

APPENDIX A: DEFINITIONS AND FEYNMAN RULES

In this Appendix we summarize definitions for various terms in the lattice actions and present Feynman rules for gauge and quark propagators and for vertex functions.

Covariant Derivatives Acting on Quark Fields

$$\nabla_\mu \Psi(x) = \frac{1}{2} \frac{1}{u_\mu} [U_\mu(x)\Psi(x+a_\mu) - U_\mu^\dagger(x-a_\mu)\Psi(x-a_\mu)] \quad (\text{A1})$$

$$\nabla_\mu^{(2)} \Psi(x) = \frac{1}{u_\mu} [U_\mu(x)\Psi(x+a_\mu) + U_\mu^\dagger(x-a_\mu)\Psi(x-a_\mu)] - 2\Psi(x) \quad (\text{A2})$$

$$\begin{aligned} \nabla_\mu^{(3)} \Psi(x) &= \frac{1}{2} \frac{1}{u_\mu^2} [U_\mu(x)U_\mu(x+a_\mu)\Psi(x+2a_\mu) - U_\mu^\dagger(x-a_\mu)U_\mu^\dagger(x-2a_\mu)\Psi(x-2a_\mu)] \\ &\quad - \frac{1}{u_\mu} [U_\mu(x)\Psi(x+a_\mu) - U_\mu^\dagger(x-a_\mu)\Psi(x-a_\mu)] \end{aligned} \quad (\text{A3})$$

$$\begin{aligned} \nabla_\mu^{(4)} \Psi(x) &= \frac{1}{u_\mu^2} [U_\mu(x)U_\mu(x+a_\mu)\Psi(x+2a_\mu) + U_\mu^\dagger(x-a_\mu)U_\mu^\dagger(x-2a_\mu)\Psi(x-2a_\mu)] \\ &\quad - 4 \frac{1}{u_\mu} [U_\mu(x)\Psi(x+a_\mu) + U_\mu^\dagger(x-a_\mu)\Psi(x-a_\mu)] + 6\Psi(x) \end{aligned} \quad (\text{A4})$$

Field Strength Tensors

For the unimproved $F_{\mu\nu}$ of the clover action we use

$$\begin{aligned} F_{\mu\nu}(x) &= \frac{1}{2i} (\Omega_{\mu\nu}(x) - \Omega_{\mu\nu}^\dagger(x)), \\ \Omega_{\mu\nu}(x) &= \frac{1}{4u_\mu^2 u_\nu^2} \sum_{\{(\alpha,\beta)\}_{\mu\nu}} U_\alpha(x)U_\beta(x+a_\alpha)U_{-\alpha}(x+a_\alpha+a_\beta)U_{-\beta}(x+a_\beta), \end{aligned} \quad (\text{A5})$$

with $\{(\alpha, \beta)\}_{\mu\nu} = \{(\mu, \nu), (\nu, -\mu), (-\mu, -\nu), (-\nu, \mu)\}$ for $\mu \neq \nu$ and $U_{-\mu}(x + a_\mu) \equiv U_\mu^\dagger(x)$. The $O(a^2)$ improved field strength tensor of the D234 actions is

$$\begin{aligned} \tilde{F}_{\mu\nu}(x) &= \frac{5}{3} F_{\mu\nu}(x) \\ &- \frac{1}{6} \left[\frac{1}{u_\mu^2} (U_\mu(x) F_{\mu\nu}(x + a_\mu) U_\mu^\dagger(x) + U_\mu^\dagger(x - a_\mu) F_{\mu\nu}(x - a_\mu) U_\mu(x - a_\mu)) - (\mu \leftrightarrow \nu) \right] \\ &+ \frac{1}{6} \left(\frac{1}{u_\mu^2} + \frac{1}{u_\nu^2} - 2 \right) F_{\mu\nu}(x). \end{aligned} \quad (\text{A6})$$

The last term ensures that factors of $1/u_\mu$ are correctly removed from those contributions to $UF_{\mu\nu}U^\dagger$ and $U^\dagger F_{\mu\nu}U$ that end up being four link objects rather than six link ones. In a one-loop calculation, however, one can set $u_\mu = 1$ everywhere in the definition of the field strength tensor and this correction term is irrelevant.

Both the above covariant derivatives and the field strength tensor are dimensionless. Factors of $1/a_t$ and $1/a_s$ are inserted explicitly where necessary such as in (6).

Gauge Propagator

The isotropic Symanzik improved gauge action has been discussed quite extensively in the literature [9]. Here we summarize formulas for the anisotropic generalization. We start from the gauge actions \mathcal{S}_G^I or \mathcal{S}_G^{II} and add to it a gauge fixing term

$$\mathcal{S}_{gf} = \frac{1}{2\alpha_g} a_s^3 a_t \sum_x \left[\frac{1}{a_t} \partial_t A_t + \frac{1}{a_s} \sum_j \partial_j A_j \right]^2 \quad (\text{A7})$$

$$= \frac{1}{2\alpha_g} \frac{1}{\chi} \sum_x \left[\chi^2 \partial_t (a_t A_t) + \sum_j \partial_j (a_s A_j) \right]^2, \quad (\text{A8})$$

with $\partial_\mu A_\mu(x) \equiv A_\mu(x + a_\mu/2) - A_\mu(x - a_\mu/2)$. Equation (A8) expresses \mathcal{S}_{gf} in terms of dimensionless gauge fields $a_\mu A_\mu$. It is convenient to do so, especially since $\mathcal{S}_G^{I,II}$ are already in dimensionless form with factors of χ and $1/\chi$ properly put in place. If $\bar{A}_\mu(k)$ is the Fourier transform of $(a_\mu A_\mu)$, the quadratic terms in the gauge action become

$$\mathcal{S}_G^{(0)I,II} + \mathcal{S}_{gf} = \frac{1}{2} \sum_{\mu\nu} \int_{-\pi}^{\pi} \frac{d^4 k}{(2\pi)^4} \left(\bar{A}_\mu(k) M_{\mu\nu}(k) \bar{A}_\nu(-k) \right), \quad (\text{A9})$$

where

$$M_{00} = \chi \left[\frac{\chi^2 \hat{k}_0^2}{\alpha_g} + \sum_j \hat{k}_j^2 q_{0j} \right] \quad (\text{A10})$$

$$M_{jj} = \frac{1}{\chi} \left[\frac{1}{\alpha_g} \hat{k}_j^2 + \chi^2 \hat{k}_0^2 q_{0j} + \sum_{l \neq j} \hat{k}_l^2 q_{lj} \right] \quad (\text{A11})$$

$$M_{i \neq j} = \frac{1}{\chi} \left[\frac{1}{\alpha_g} \hat{k}_i \hat{k}_j - \hat{k}_i \hat{k}_j q_{ij} \right] \quad (\text{A12})$$

$$M_{0j} = M_{j0} = \chi \left[\frac{1}{\alpha_g} \hat{k}_0 \hat{k}_j - \hat{k}_0 \hat{k}_j q_{0j} \right] \quad (\text{A13})$$

and

$$\hat{k}_\mu \equiv 2 \sin\left(\frac{k_\mu}{2}\right). \quad (\text{A14})$$

The $q_{\mu\nu}$ need to be specified only for $\mu \neq \nu$ and one has

$$q_{\mu\nu} = 1 - c_1^G (\hat{k}_\mu^2 + \hat{k}_\nu^2) \quad \mu \neq \nu \quad \mathcal{S}_G^I \quad (\text{A15})$$

$$q_{ij} = 1 + \frac{1}{12} (\hat{k}_i^2 + \hat{k}_j^2) \quad i \neq j \quad \mathcal{S}_G^{II}$$

$$q_{0j} = 1 + \frac{1}{12} \hat{k}_j^2 \quad \mathcal{S}_G^{II} \quad (\text{A16})$$

We have inverted the 4×4 matrix $M_{\mu\nu}$ using Mathematica keeping $q_{\mu\nu}$ general. For both gauge actions, \mathcal{S}_G^I and \mathcal{S}_G^{II} the free gauge propagator has the structure

$$D_{\mu\nu}(k) = M_{\mu\nu}^{-1} = \frac{1}{(\hat{k}^2)^2} \left[\alpha_g \hat{k}_\mu \hat{k}_\nu \chi + \frac{f_N^{\mu\nu}(\hat{k}_\rho, q_{\rho\sigma}, \chi)}{f_D(\hat{k}_\rho, q_{\rho\sigma}, \chi)} \right], \quad (\text{A17})$$

with

$$\hat{k}^2 = \chi^2 k_0^2 + \sum_j \hat{k}_j^2. \quad (\text{A18})$$

The term proportional to the gauge fixing parameter α_g has the familiar form

$$\alpha_g \frac{\hat{k}_\mu \hat{k}_\nu}{(\hat{k}^2)^2} \chi = \alpha_g \frac{a_\mu a_\nu}{a_s^3 a_t} \frac{\hat{k}_\mu \hat{k}_\nu / (a_\mu a_\nu)}{[(\hat{k}_0/a_t)^2 + \sum_j (\hat{k}_j/a_s)^2]^2} \quad (\text{A19})$$

with the conversion factor $a_\mu a_\nu / a_s^3 a_t$ mentioned in (57). This factor results because we are looking at the propagator for dimensionless gauge fields $a_\mu A_\mu$ and because we carried out a dimensionless Fourier transform. The second term in (A17) is much more complicated. If one writes

$$f_N^{00}(\hat{k}_\rho, q_{\rho\sigma}, \chi) = \frac{1}{\chi} \tilde{f}_N^{00} \quad (\text{A20})$$

$$f_N^{jj}(\hat{k}_\rho, q_{\rho\sigma}, \chi) = \chi \tilde{f}_N^{jj} \quad (\text{A21})$$

$$f_N^{i \neq j}(\hat{k}_\rho, q_{\rho\sigma}, \chi) = \chi \hat{k}_i \hat{k}_j \tilde{f}_N^{i \neq j} \quad (\text{A22})$$

$$f_N^{0j}(\hat{k}_\rho, q_{\rho\sigma}, \chi) = \chi \hat{k}_0 \hat{k}_j \tilde{f}_N^{0j} \quad (\text{A23})$$

one can show that f_D and all the $\tilde{f}_N^{\mu\nu}$ are functions only of $(\chi \hat{k}_0)^2, \hat{k}_j^2, q_{\rho\sigma}$ with no other χ dependence or odd powers of \hat{k}_ρ . We have not shown color indices in the above expressions. The gluon propagator is diagonal in color.

Quark Propagator

The inverse free quark propagator for \mathcal{S}_{D234}^I is given by

$$a_t \overline{G}_0^{-1}(k) = i\gamma_0 K_0(k_0) \sin(k_0) + i\frac{C_0}{\chi} \sum_j \gamma_j K_j(k_j) \sin(k_j) + \Omega(k_0, \vec{k}) \quad (\text{A24})$$

with

$$K_0 = 1 + \frac{C_{3t}}{3} - \frac{C_{3t}}{3} \cos(k_0) \quad (\text{A25})$$

$$K_j = 1 + \frac{C_3}{3} - \frac{C_3}{3} \cos(k_j) \quad (\text{A26})$$

and

$$\begin{aligned} \Omega = \chi & \left[2\left(1 + \frac{C_{4t}}{3}\right) \sin^2\left(\frac{k_0}{2}\right) - \frac{C_{4t}}{6} \sin^2(k_0) \right] \\ & \frac{1}{\chi} \sum_j \left[2\left(1 + \frac{C_4}{3}\right) \sin^2\left(\frac{k_j}{2}\right) - \frac{C_4}{6} \sin^2(k_j) \right] + a_t m. \end{aligned} \quad (\text{A27})$$

Propagators for the other quark actions can be obtained by setting the appropriate $C_{i(t)}$ equal to zero. Quark propagators are diagonal in color.

Vertex Functions

In deriving the one- and two-gluon emission vertices we have used the method described in [22]. We list again results only for \mathcal{S}_{D234}^I . Those for other quark actions follow trivially. The general form for a single gluon emission vertex is

$$V_\mu(k', k) \equiv -i\gamma_\mu W_\mu - W'_\mu - \sum_\nu \sigma_{\nu\mu} W''_{\nu\mu} \quad (\text{A28})$$

where μ is the polarization of the emitted gluon, k' the momentum of the outgoing quark and k the momentum of the incoming quark. We suppress the color factor T_{bc}^a which should multiply each of the above terms. Using the variables

$$k_\mu^\pm \equiv \frac{1}{2}(k' \pm k)_\mu \quad (\text{A29})$$

one has

$$W_0 = \left(1 + \frac{C_{3t}}{3}\right) \cos(k_0^+) - \frac{C_{3t}}{3} \cos(2k_0^+) \cos(k_0^-) \quad (\text{A30})$$

$$W_j = \frac{C_0}{\chi} \left[\left(1 + \frac{C_3}{3}\right) \cos(k_j^+) - \frac{C_3}{3} \cos(2k_j^+) \cos(k_j^-) \right] \quad (\text{A31})$$

$$W'_0 = \chi \left[\left(1 + \frac{C_{4t}}{3}\right) \sin(k_0^+) - \frac{C_{4t}}{6} \sin(2k_0^+) \cos(k_0^-) \right] \quad (\text{A32})$$

$$W'_j = \frac{1}{\chi} \left[\left(1 + \frac{C_4}{3}\right) \sin(k_j^+) - \frac{C_4}{6} \sin(2k_j^+) \cos(k_j^-) \right] \quad (\text{A33})$$

and

$$W''_{j0} = \frac{1}{2} \sin(2k_j^-) \cos(k_0^-) \frac{1}{3} [5 - \cos(2k_j^-) - \cos(2k_0^-)] \quad (\text{A34})$$

$$W''_{0j} = \frac{1}{2} \sin(2k_0^-) \cos(k_j^-) \frac{1}{3} [5 - \cos(2k_j^-) - \cos(2k_0^-)] \quad (\text{A35})$$

$$W''_{ij} = \frac{1}{2} \frac{1}{\chi} \sin(2k_i^-) \cos(k_j^-) \frac{1}{3} [5 - \cos(2k_i^-) - \cos(2k_j^-)]. \quad (\text{A36})$$

For the clover action the factor $\frac{1}{3}[5 - \cos(2k_\mu^-) - \cos(2k_\nu^-)]$ in $W''_{\mu\nu}$ should be replaced by 1.

For the two-gluon emission vertex we do not present the most general result, but restrict ourselves to those terms necessary for the tadpole diagram Σ^{tad} . For instance, the $\sigma_{\mu\nu} F_{\mu\nu}$ term does not contribute to the tadpole diagram. We also omit terms that vanish upon symmetrizing between the two gluons. If $V_{\mu_1\mu_2}^{(2)}(k', k, q_1, q_2)$ stands for the emission vertex for gluons of momentum q_i and polarization μ_i , with $k_\mu = k'_\mu + q_{1,\mu} + q_{2,\mu}$, one has

$$\begin{aligned} V_{00}^{(2)} = & \frac{i}{2} \gamma_0 \left[\left(1 + \frac{C_{3t}}{3}\right) \sin(k_0^+) - \frac{2}{3} C_{3t} \sin(2k_0^+) \cos\left(\frac{q_{1,0}}{2}\right) \cos\left(\frac{q_{2,0}}{2}\right) \right] \\ & - \frac{\chi}{2} \left[\left(1 + \frac{C_{4t}}{3}\right) \cos(k_0^+) - \frac{1}{3} C_{4t} \cos(2k_0^+) \cos\left(\frac{q_{1,0}}{2}\right) \cos\left(\frac{q_{2,0}}{2}\right) \right] \end{aligned} \quad (\text{A37})$$

$$\begin{aligned} V_{jj}^{(2)} = & \frac{i}{2} \frac{C_0}{\chi} \gamma_j \left[\left(1 + \frac{C_3}{3}\right) \sin(k_j^+) - \frac{2}{3} C_3 \sin(2k_j^+) \cos\left(\frac{q_{1,j}}{2}\right) \cos\left(\frac{q_{2,j}}{2}\right) \right] \\ & - \frac{1}{2\chi} \left[\left(1 + \frac{C_4}{3}\right) \cos(k_j^+) - \frac{1}{3} C_4 \cos(2k_j^+) \cos\left(\frac{q_{1,j}}{2}\right) \cos\left(\frac{q_{2,j}}{2}\right) \right]. \end{aligned} \quad (\text{A38})$$

The color factor for these vertex functions is $(T^{a_1} T^{a_2})_{bc}$.

APPENDIX B: IR SUBTRACTIONS

In this Appendix we list the IR subtraction, \mathcal{F}_{sub} of equation (61), necessary to control numerical integration of IR divergent integrals. A gluon mass, λ/a_s , is introduced into $D_{\mu\nu}$ by replacing the first factor in (A17) by

$$\frac{1}{(\hat{k}^2)^2} \rightarrow \frac{1}{\hat{k}^2} \frac{1}{\hat{k}^2 + \lambda^2}. \quad (\text{B1})$$

The lattice wave function renormalization Z_2 must reproduce the same IR divergence structure as in continuum QCD. For Z_2^{-1} at one-loop the IR divergence is

$$\begin{aligned} \frac{\alpha_s}{3\pi} [-1 - (\alpha_g - 1)] \ln(\lambda^2) & \quad m = 0 \\ \frac{\alpha_s}{3\pi} [2 - (\alpha_g - 1)] \ln(\lambda^2) & \quad m > 0 \end{aligned} \quad (\text{B2})$$

We note that by the $m = 0$ theory we mean one in which the quark mass has been set to zero before taking the limit $\lambda \rightarrow 0$. This is the usual practice in much of the literature on

massless lattice perturbation theory. Alternatively one could take the limit $am \rightarrow 0$ and $\lambda \rightarrow 0$ keeping $am \geq \lambda$. Since we want to compare with some of the massless literature with improved glue actions (e.g. [12]) we adopt the first definition in this article. In our massive calculations we do not go to extremely small masses and have not attempted to isolate $\ln(am)$ contributions.

For our VEGAS integrations it was convenient to separate the d/dp_0 derivative in (61) into two parts

$$\frac{d}{dp_0} \left[V_\mu \frac{\bar{G}_0}{a_t} V_\nu \right] \equiv \frac{d}{dp_0} \left[\frac{VGV_{num}}{VGV_{den}} \right] = \frac{VGV'_{num}}{VGV_{den}} - \frac{VGV_{num}}{(VGV_{den})^2} VGV'_{den}. \quad (\text{B3})$$

Corresponding to the two parts with derivatives acting on the numerator or denominator, respectively, we introduce two separate subtraction terms \mathcal{F}_{sub}^{num} and \mathcal{F}_{sub}^{den} . These are obtained by calculating the self energy diagram in continuum Euclidean perturbation theory with an appropriate mass m_{eff} and the mass-shell condition $p = (i m_{eff}, \vec{0})$. The effective mass follows from expanding the lattice integrand in (61) about small k and comparing with the continuum calculation [13]. It is given in (64). After converting to the dimensionless integration variables k_μ of (61) one has for the part with the derivative acting on the denominator

$$\begin{aligned} \mathcal{F}_{sub}^{den} &= \theta(\Lambda^2 - k^2) \\ &\times \left\{ \frac{-4\chi(\chi^2 k_0^2 + b^2/4)((k^2)^2 - b^2\chi^2 k_0^2)}{(k^2 + \lambda^2)((k^2)^2 + b^2\chi^2 k_0^2)^2} + (\alpha_g - 1)\chi \frac{\chi^2 k_0^2(b^2 + 2k^2)}{k^2(k^2 + \lambda^2)((k^2)^2 + b^2\chi^2 k_0^2)} \right\}, \end{aligned} \quad (\text{B4})$$

with

$$k^2 = \chi^2 k_0^2 + \sum_j k_j^2 \quad b = 2a_s m_{eff}. \quad (\text{B5})$$

The θ -function imposes a cutoff on \mathcal{F}_{sub}^{den} so that it vanishes identically for $k^2 > \Lambda^2$, where Λ is some number $0 < \Lambda \leq \pi$. The subtraction term can be integrated analytically to give

$$\begin{aligned} F^{den}(m_{eff} > 0, \Lambda, \lambda) &= \int_k \mathcal{F}_{sub}^{den}(k, m_{eff} > 0, \Lambda, \lambda) \\ &= \frac{\alpha_s}{3\pi} \left\{ \left[-2 \ln\left(\frac{\Lambda^2}{\lambda^2}\right) + 2 \ln\left(\frac{\Lambda + \sqrt{b^2 + \Lambda^2}}{b}\right) + \frac{4\Lambda^2}{b^4}(b^2 + 3\Lambda^2) + \frac{\sqrt{b^2 + \Lambda^2}}{b^4} 2\Lambda(b^2 - 6\Lambda^2) \right] \right. \\ &\quad \left. + (\alpha_g - 1) \left[\ln\left(\frac{\Lambda^2}{\lambda^2}\right) + \frac{2\Lambda^2}{b^4}(\Lambda^2 + 2b^2) - \frac{\Lambda(2\Lambda^2 + 3b^2)}{b^4} \sqrt{b^2 + \Lambda^2} - \ln\left(\frac{\Lambda + \sqrt{b^2 + \Lambda^2}}{b}\right) \right] \right\} \end{aligned} \quad (\text{B6})$$

and

$$F^{den}(m_{eff} \equiv 0, \Lambda, \lambda) = \frac{\alpha_s}{3\pi} \left[-1 + \frac{\alpha_g - 1}{2} \right] \ln\left(\frac{\Lambda^2}{\lambda^2}\right). \quad (\text{B7})$$

The contribution in (B3) from the derivative acting on the numerator is

$$\mathcal{F}_{sub}^{num} = \theta(\Lambda^2 - k^2) \left\{ \frac{2\chi k^2}{((k^2)^2 + b^2\chi^2 k_0^2)(k^2 + \lambda^2)} + (\alpha_g - 1)\chi \frac{k^2 - 2\chi^2 k_0^2}{((k^2)^2 + b^2\chi^2 k_0^2)(k^2 + \lambda^2)} \right\}, \quad (\text{B8})$$

which leads to

$$\begin{aligned} F^{num}(m_{eff} > 0, \Lambda, \lambda) &= \int_k \mathcal{F}_{sub}^{num}(k, m_{eff} > 0, \Lambda, \lambda) \\ &= \frac{\alpha_s}{3\pi} \left\{ \left[4 \ln \left(\frac{\Lambda + \sqrt{b^2 + \Lambda^2}}{b} \right) - \frac{4\Lambda^2}{b^2} + \frac{4\Lambda}{b^2} \sqrt{b^2 + \Lambda^2} \right] \right. \\ &\quad \left. + (\alpha_g - 1) \left[\ln \left(\frac{\Lambda + \sqrt{b^2 + \Lambda^2}}{b} \right) - \frac{2\Lambda^2}{b^4} (\Lambda^2 + 2b^2) + \frac{\Lambda(2\Lambda^2 + 3b^2)}{b^4} \sqrt{b^2 + \Lambda^2} \right] \right\} \quad (\text{B9}) \end{aligned}$$

and

$$F^{num}(m_{eff} \equiv 0, \Lambda, \lambda) = \frac{\alpha_s}{3\pi} \left[2 + \frac{\alpha_g - 1}{2} \right] \ln \left(\frac{\Lambda^2}{\lambda^2} \right). \quad (\text{B10})$$

$F^{den} + F^{num}$ reproduces the IR divergent logarithms of (B2).

REFERENCES

- [1] C. Morningstar and M. Peardon; Phys. Rev. D**60**:034509 (1999).
- [2] T. Manke et al.; Phys. Rev. Lett **82**:4396 (1999).
- [3] I. Drummond et al.; hep-lat/9912041.
- [4] CP-PACS Collaboration, T. Manke et al.; hep-lat/9909038.
- [5] B. Mertens, A. Kronfeld and A. El-Khadra; Phys. Rev. D**58**: 034505 (1998).
- [6] M. Alford, T. Klassen and G. P. Lepage; Phys. Rev. D**58**:034503 (1998), Nucl. Phys. B**496** 377 (1997).
- [7] G.P. Lepage; Nucl. Phys. B (Proc. Suppl.)**60A** 267 (1998).
- [8] G.P. Lepage and P.B. Mackenzie, Phys. Rev. D**48**, 2250 (1993).
- [9] P. Weisz; Nucl. Phys. B**212** 1 (1983); P. Weisz and R. Wohlert; Nucl. Phys. B**236** 397 (1984) ; erratum, *ibid.* B**247** 544 (1984).
- [10] Y. Iwasaki, preprint, UTHEP-118 (Dec. 1983), unpublished.
- [11] B. Sheikholeslami and R. Wohlert, Nucl. Phys. B**259**, 572 (1985).
- [12] S. Aoki et al.; Phys. Rev. D**58**:074505 (1998).
- [13] Y. Kuramashi; Phys. Rev. D**58**:034507 (1998).
- [14] M. Lüscher; Comm. Math. Phys. **54** 283 (1977).
- [15] A. El-Khadra, A. Kronfeld and P. Mackenzie; Phys. Rev. D**55** 3933 (1997).
- [16] G.P. Lepage, J. Comput. Phys. **27**, 192 (1978).
- [17] E. Eichten and B. Hill; Phys. Lett. B**240**, 193 (1990).
- [18] M. Alford, T. Klassen and G.P. Lepage; Nucl. Phys. B(Proc.Suppl)**53**, 861 (1997)
- [19] M. Alford, R. Horgan et al.; in preparation.
- [20] P. Bouchard, C. Lin and O. Pene; Phys. Rev. D**40**, 1529 (1989); D**41**, 3541(E) (1990).
- [21] A. Borrelli and C. Pittori; Nucl. Phys. B**385**, 502 (1992).
- [22] C. Morningstar; Phys. Rev. D**48**, 2265 (1993).

TABLES

action	comments	parameters
$\mathcal{S}^A = \mathcal{S}_G^I + \mathcal{S}_{clover}$	massive and massless	$c_0^G = 5/3, c_1^G = -1/12, \chi = 1$
$\mathcal{S}^{A'} = \mathcal{S}_G^I + \mathcal{S}_{clover}$	massive and massless	$c_0^G = 3.648, c_1^G = -0.331, \chi = 1$
$\mathcal{S}^B = \mathcal{S}_G^{II} + \mathcal{S}_{clover}$	massive and massless	$\chi \geq 1$
$\mathcal{S}^C = \mathcal{S}_G^I + \mathcal{S}_{D234}^I$	massless	$c_0^G = 5/3, c_1^G = -1/12, \chi = 1$
$\mathcal{S}^D = \mathcal{S}_G^{II} + \mathcal{S}_{D234}^{II}$	massive and massless	$\chi \geq 1$

TABLE I. Combinations of gauge and quark actions considered in this article.

Action \mathcal{S}^A						
$a_s M_1^{(0)}$	regular	tadpole	reg + tad	t.i.	$a_s M_{1,nosub}^{(1)}$	$a_s M_{1,sub}^{(1)}$
	$\alpha_g = 1.0$					
0.00	-1.770(3)	4.298	2.528(3)	-3.001	-0.472(3)	0.000
0.01	-1.718(5)	4.266	2.548(5)	-2.978	-0.430(5)	0.037(6)
0.05	-1.547(3)	4.141	2.594(3)	-2.891	-0.297(3)	0.152(4)
0.10	-1.369(3)	3.991	2.623(3)	-2.786	-0.164(3)	0.263(4)
0.50	-0.463(3)	3.030	2.567(3)	-2.115	0.451(3)	0.737(3)
1.00	0.092(3)	2.260	2.352(3)	-1.578	0.774(3)	0.948(3)
2.00	0.530(3)	1.511	2.041(3)	-1.055	0.986(3)	1.050(3)
5.00	0.743(3)	1.096	1.839(3)	-0.765	1.074(3)	1.077(3)
10.00	0.752(3)	1.075	1.827(3)	-0.750	1.077(3)	1.077(3)
	$\alpha_g = 0.0$					
0.00	-0.472(3)	3.001	2.528(3)	-3.001	-0.472(3)	0.000
0.01	-0.429(5)	2.978	2.549(5)	-2.978	-0.429(5)	0.038(6)
0.05	-0.293(3)	2.891	2.597(3)	-2.891	-0.293(3)	0.156(4)
0.10	-0.161(3)	2.786	2.626(3)	-2.786	-0.161(3)	0.266(4)
0.50	0.454(3)	2.115	2.569(3)	-2.115	0.454(3)	0.740(3)
1.00	0.775(3)	1.578	2.353(3)	-1.578	0.775(3)	0.949(3)
2.00	0.987(3)	1.055	2.042(3)	-1.055	0.987(3)	1.051(3)
5.00	1.076(3)	0.765	1.841(3)	-0.765	1.076(3)	1.079(3)
10.00	1.079(3)	0.750	1.829(3)	-0.750	1.079(3)	1.079(3)

TABLE II. One-loop mass renormalization for action \mathcal{S}^A for different $a_s M_1^{(0)}$ values. Results are presented for two choices of the gauge parameter $\alpha_g = 1$ and $\alpha_g = 0$. $a_s M_{1,nosub}^{(1)}$ is the same as (reg + tad + t.i.). $a_s M_{1,sub}^{(1)}$ is defined in (40) and related to $a_s M_{1,nosub}^{(1)}$ in (78). Where errors are not indicated explicitly, they are of $O(1)$ or less in the last digit.

$a_s M_1^{(0)}$	Action $\mathcal{S}^{A'}$			Action \mathcal{S}^C		
	reg + tad	$a_s M_{1,nosub}^{(1)}$	$a_s M_{1,sub}^{(1)}$	reg + tad	$a_s M_{1,nosub}^{(1)}$	$a_s M_{1,sub}^{(1)}$
0.00	1.480	-0.397	0.000	2.213	-1.287	0.000
0.01	1.505	-0.358	0.035			
0.05	1.566	-0.242	0.136			
0.10	1.612	-0.131	0.228			
0.50	1.690	0.367	0.608			
1.00	1.611	0.624	0.770			
2.00	1.466	0.806	0.859			
5.00	1.376	0.897	0.900			
10.00	1.371	0.901	0.901			

TABLE III. One-loop mass renormalization for actions $\mathcal{S}^{A'}$ and \mathcal{S}^C . Numerical integration errors are at the ± 0.006 level for $a_s M_1^{(0)} = 0.01$ and of $O(4)$ or less in the last digit otherwise.

Action \mathcal{S}^B						
	reg + tad	$a_s M_{1,nosub}^{(1)}$	$a_s M_{1,sub}^{(1)}$	reg + tad	$a_s M_{1,nosub}^{(1)}$	$a_s M_{1,sub}^{(1)}$
$a_s M_1^{(0)}$	$\chi = 1.0$			$\chi = 2.0$		
0.00	2.710	-0.479	0.000	3.240	-0.881	0.000
0.01	2.729	-0.436	0.038	3.250	-0.833	0.039
0.05	2.774	-0.299	0.157	3.260	-0.675	0.164
0.10	2.799	-0.164	0.269	3.251	-0.512	0.288
0.50	2.717	0.463	0.754	3.060	0.290	0.863
1.00	2.466	0.779	0.955	2.824	0.772	1.178
2.00	2.096	0.961	1.026	2.461	1.155	1.381
5.00	1.842	1.014	1.017	1.978	1.371	1.419
$a_s M_1^{(0)}$	$\chi = 3.0$			$\chi = 3.6$		
0.00	3.298	-1.139	0.000	3.286	-1.243	0.000
0.01	3.302	-1.092	0.036	3.289	-1.195	0.036
0.05	3.312	-0.918	0.167	3.299	-1.017	0.167
0.10	3.299	-0.742	0.293	3.287	-0.835	0.295
0.50	3.110	0.145	0.896	3.106	0.083	0.905
1.00	2.901	0.695	1.244	2.910	0.656	1.262
2.00	2,589	1.161	1.498	2.620	1.151	1.532
5.00	2.106	1.472	1.582	2.158	1.496	1.636
$a_s M_1^{(0)}$	$\chi = 4.0$			$\chi = 5.0$		
0.00	3.271	-1.299	0.000	3.233	-1.405	0.000
0.01	3.271	-1.255	0.031	3.233	-1.360	0.031
0.05	3.285	-1.070	0.167	3.249	-1.170	0.168
0.10	3.274	-0.885	0.296	3.239	-0.980	0.297
0.50	3.099	0.049	0.910	3.076	-0.018	0.915
1.00	2.911	0.634	1.270	2.903	0.590	1.283
2.00	2.631	1.143	1.547	2.645	1.124	1.572
5.00	2.184	1.505	1.662	2.228	1.518	1.707
$a_s M_1^{(0)}$	$\chi = 5.3$			$\chi = 6.0$		
0.00	3.222	-1.429	0.000	3.197	-1.479	0.000
0.01	3.226	-1.380	0.035	3.204	-1.426	0.038
0.05	3.238	-1.194	0.167	3.213	-1.241	0.168
0.10	3.228	-1.003	0.296	3.205	-1.048	0.296
0.50	3.069	-0.034	0.915	3.053	-0.065	0.918
1.00	2.899	0.579	1.285	2.891	0.557	1.290
2.00	2.647	1.119	1.577	2.649	1.108	1.586
5.00	2.237	1.520	1.717	2.254	1.522	1.734

TABLE IV. One-loop mass renormalization for action \mathcal{S}^B for several values of the anisotropy $\chi = a_s/a_t$. Numerical integration errors are as in Table III.

Action \mathcal{S}^D						
	reg + tad	$a_s M_{1,nosub}^{(1)}$	$a_s M_{1,sub}^{(1)}$	reg + tad	$a_s M_{1,nosub}^{(1)}$	$a_s M_{1,sub}^{(1)}$
$a_s M_1^{(0)}$	$\chi = 1.0$			$\chi = 2.0$		
0.00	2.247	-1.339	0.000	2.740	-1.927	0.000
0.01	2.268	-1.289	0.037	2.744	-1.878	0.030
0.05	2.329	-1.121	0.153	2.776	-1.678	0.157
0.10	2.375	-0.947	0.265	2.785	-1.473	0.277
0.50	2.451	-0.043	0.769	2.728	-0.396	0.858
1.00	2.342	0.510	1.003	2.623	0.320	1.208
2.00	2.082	0.894	1.075	2.404	0.958	1.453
5.00	1.843	1.012	1.021	1.986	1.349	1.455
$a_s M_1^{(0)}$	$\chi = 3.0$			$\chi = 3.6$		
0.00	2.788	-2.250	0.000	2.777	-2.370	0.000
0.01	2.794	-2.195	0.033	2.781	-2.315	0.032
0.05	2.818	-1.984	0.159	2.805	-2.099	0.158
0.10	2.824	-1.762	0.282	2.811	-1.872	0.282
0.50	2.759	-0.601	0.883	2.751	-0.680	0.888
1.00	2.674	0.178	1.262	2.675	0.120	1.275
2.00	2.506	0.901	1.566	2.528	0.870	1.596
5.00	2.115	1.423	1.639	2.166	1.435	1.701
$a_s M_1^{(0)}$	$\chi = 4.0$			$\chi = 5.0$		
0.00	2.769	-2.427	0.000	2.732	-2.544	0.000
0.01	2.768	-2.377	0.026	2.734	-2.490	0.029
0.05	2.792	-2.152	0.159	2.760	-2.267	0.156
0.10	2.799	-1.928	0.278	2.768	-2.030	0.282
0.50	2.742	-0.722	0.886	2.719	-0.798	0.891
1.00	2.672	0.090	1.279	2.660	0.033	1.288
2.00	2.536	0.853	1.609	2.542	0.817	1.629
5.00	2.190	1.436	1.729	2.232	1.436	1.779
$a_s M_1^{(0)}$	$\chi = 5.3$			$\chi = 6.0$		
0.00	2.720	-2.572	0.000	2.701	-2.620	0.000
0.01	2.724	-2.516	0.031	2.708	-2.561	0.033
0.05	2.759	-2.283	0.166	2.732	-2.337	0.158
0.10	2.765	-2.047	0.291	2.740	-2.099	0.283
0.50	2.717	-0.810	0.899	2.699	-0.848	0.894
1.00	2.658	0.022	1.293	2.646	-0.007	1.291
2.00	2.543	0.809	1.633	2.541	0.791	1.638
5.00	2.242	1.436	1.791	2.256	1.432	1.808

TABLE V. One-loop mass renormalization for action \mathcal{S}^D for several values of the anisotropy $\chi = a_s/a_t$. Numerical integration errors are as in Table III.

Action \mathcal{S}^A						
$a_s M_1^{(0)}$	$\alpha_g = 1.0$			$\alpha_g = 0.0$		
	$Z_{2,dp_0}^{(1)}$ no $t.i.$	$Z_{2,dp_0}^{(1)}$ with $t.i.$	$Z_2^{(1)}$ with $t.i.$	$Z_{2,dp_0}^{(1)}$ no $t.i.$	$Z_{2,dp_0}^{(1)}$ with $t.i.$	$Z_2^{(1)}$ with $t.i.$
0.00	0.687(3)	-0.063(3)	-0.063(3)	1.195(3)	0.445(3)	0.445(3)
0.01	-2.688(6)	-3.438(6)	-3.475(7)	-2.169(6)	-2.919(6)	-2.956(7)
0.05	-1.569(5)	-2.319(5)	-2.471(6)	-1.052(5)	-1.802(5)	-1.954(6)
0.10	-1.041(5)	-1.791(5)	-2.054(6)	-0.524(5)	-1.274(5)	-1.537(6)
0.50	0.393(3)	-0.357(3)	-1.094(4)	0.905(3)	0.155(3)	-0.582(4)
1.00	1.112(3)	0.362(3)	-0.586(4)	1.623(3)	0.873(3)	-0.075(4)
2.00	1.795(3)	1.045(3)	-0.005(4)	2.304(3)	1.554(3)	0.504(4)
5.00	2.223(20)	1.473(20)	0.396(20)	2.719(20)	1.969(20)	0.892(20)

TABLE VI. One-loop wave function renormalization for action \mathcal{S}^A for different $a_s M_1^{(0)}$ values. Results are presented for two choices for the gauge parameter $\alpha_g = 1$ and $\alpha_g = 0$. $Z_2^{(1)}$ includes both $Z_{2,dp_0}^{(1)}$ and $Z_{2,M_1}^{(1)}$ as defined in equation (82).

$a_s M_1^{(0)}$	Action \mathcal{S}^A $\alpha_g = 1.0$	
	$Z_{2,diff}^{(1)}$ no $t.i.$	$Z_{2,diff}^{(1)}$ with $t.i.$
0.00	0.634(3)	-0.116(3)
0.01	0.668(6)	-0.082(6)
0.05	0.763(5)	0.013(5)
0.10	0.849(5)	0.099(5)
0.50	1.259(3)	0.509(3)
1.00	1.536(3)	0.786(3)
2.00	1.778(3)	1.028(3)
5.00	1.623(20)	0.873(20)

TABLE VII. $Z_{2,dp_0}^{(1)}$ with $\ln(am)$ contributions subtracted out for action \mathcal{S}^A in Feynman gauge. $Z_{2,diff}^{(1)}$ is defined in equation (84).

Action $\mathcal{S}^{A'}$						
$a_s M_1^{(0)}$	$\alpha_g = 1.0$			$\alpha_g = 0.0$		
	$Z_{2,dp_0}^{(1)}$ no <i>t.i.</i>	$Z_{2,dp_0}^{(1)}$ with <i>t.i.</i>	$Z_2^{(1)}$ with <i>t.i.</i>	$Z_{2,dp_0}^{(1)}$ no <i>t.i.</i>	$Z_{2,dp_0}^{(1)}$ with <i>t.i.</i>	$Z_2^{(1)}$ with <i>t.i.</i>
0.00	0.239	-0.230	-0.230	0.747	0.278	0.278
0.01	-3.137	-3.606	-3.641	-2.628	-3.097	-3.132
0.05	-2.024	-2.493	-2.629	-1.515	-1.984	-2.120
0.10	-1.502	-1.971	-2.199	-0.993	-1.462	-1.690
0.50	-0.120	-0.590	-1.198	0.389	-0.081	-0.689
1.00	0.546	0.076	-0.694	1.054	0.585	-0.185
2.00	1.165	0.695	-0.164	1.674	1.204	0.345
5.00	1.568	1.099	0.199	2.079	1.610	0.710

Action \mathcal{S}^C						
$a_s M_1^{(0)}$	$\alpha_g = 1.0$			$\alpha_g = 0.0$		
	$Z_{2,dp_0}^{(1)}$ no <i>t.i.</i>	$Z_{2,dp_0}^{(1)}$ with <i>t.i.</i>	$Z_2^{(1)}$ with <i>t.i.</i>	$Z_{2,dp_0}^{(1)}$ no <i>t.i.</i>	$Z_{2,dp_0}^{(1)}$ with <i>t.i.</i>	$Z_2^{(1)}$ with <i>t.i.</i>
0.00	0.145	-0.355	-0.355	0.653	0.153	0.153

TABLE VIII. One-loop wave function renormalization for actions $\mathcal{S}^{A'}$ and \mathcal{S}^C . Numerical integration errors are at the ± 0.02 level for $a_s M_1^{(0)} = 5.0$, at the ± 0.006 level for $a_s M_1^{(0)} = 0.01$, 0.05 and 0.10 and of $O(4)$ in the last digit for other masses.

Action \mathcal{S}^B $\alpha_g = 1.0$						
	$Z_{2,dp_0}^{(1)}$ no <i>t.i.</i>	$Z_{2,dp_0}^{(1)}$ with <i>t.i.</i>	$Z_2^{(1)}$ with <i>t.i.</i>	$Z_{2,dp_0}^{(1)}$ no <i>t.i.</i>	$Z_{2,dp_0}^{(1)}$ with <i>t.i.</i>	$Z_2^{(1)}$ with <i>t.i.</i>
$a_s M_1^{(0)}$	$\chi = 1.0$			$\chi = 2.0$		
0.00	0.789	-0.023	-0.023	0.323	0.110	0.110
0.01	-2.586	-3.398	-3.431	-3.050	-3.263	-3.293
0.05	-1.469	-2.281	-2.437	-1.930	-2.143	-2.301
0.10	-0.942	-1.755	-2.024	-1.406	-1.619	-1.887
0.50	0.467	-0.345	-1.099	-0.111	-0.324	-0.974
1.00	1.150	0.337	-0.618	0.398	0.185	-0.569
2.00	1.766	0.953	-0.073	0.822	0.609	-0.147
5.00	2.124	1.312	0.295	1.237	1.025	0.312
$a_s M_1^{(0)}$	$\chi = 3.0$			$\chi = 3.6$		
0.00	0.265	0.172	0.172	0.253	0.190	0.190
0.01	-3.107	-3.200	-3.231	-3.118	-3.182	-3.213
0.05	-1.988	-2.080	-2.240	-1.999	-2.062	-2.222
0.10	-1.465	-1.558	-1.828	-1.476	-1.540	-1.810
0.50	-0.198	-0.290	-0.923	-0.216	-0.279	-0.907
1.00	0.259	0.167	-0.534	0.228	0.165	-0.522
2.00	0.594	0.501	-0.150	0.536	0.473	-0.147
5.00	0.911	0.819	0.272	0.807	0.744	0.256
$a_s M_1^{(0)}$	$\chi = 4.0$			$\chi = 5.0$		
0.00	0.249	0.198	0.198	0.242	0.210	0.210
0.01	-3.123	-3.174	-3.205	-3.130	-3.162	-3.193
0.05	-2.003	-2.054	-2.214	-2.010	-2.042	-2.202
0.10	-1.481	-1.532	-1.803	-1.487	-1.519	-1.790
0.50	-0.223	-0.275	-0.901	-0.233	-0.266	-0.889
1.00	0.215	0.164	-0.517	0.196	0.164	-0.508
2.00	0.511	0.460	-0.146	0.473	0.441	-0.143
5.00	0.758	0.707	0.249	0.678	0.645	0.236
$a_s M_1^{(0)}$	$\chi = 5.3$			$\chi = 6.0$		
0.00	0.241	0.212	0.212	0.238	0.216	0.216
0.01	-3.131	-3.160	-3.191	-3.133	-3.156	-3.186
0.05	-2.011	-2.040	-2.200	-2.013	-2.036	-2.196
0.10	-1.488	-1.517	-1.788	-1.490	-1.513	-1.783
0.50	-0.236	-0.264	-0.887	-0.239	-0.261	-0.882
1.00	0.193	0.164	-0.506	0.186	0.164	-0.502
2.00	0.466	0.437	-0.142	0.453	0.431	-0.140
5.00	0.661	0.633	0.234	0.631	0.609	0.229

TABLE IX. One-loop wave function renormalization for action \mathcal{S}^D in Feynman gauge. Numerical integration errors are at the ± 0.02 level for $a_s M_1^{(0)} = 5.0$ and $\chi < 3$, at the ± 0.006 level for $a_s M_1^{(0)} = 0.01, 0.05$ and 0.10 and of $O(4)$ in the last digit for all other cases.

Action \mathcal{S}^B $\alpha_g = 0.0$						
	$Z_{2,dp_0}^{(1)}$ no <i>t.i.</i>	$Z_{2,dp_0}^{(1)}$ with <i>t.i.</i>	$Z_2^{(1)}$ with <i>t.i.</i>	$Z_{2,dp_0}^{(1)}$ no <i>t.i.</i>	$Z_{2,dp_0}^{(1)}$ with <i>t.i.</i>	$Z_2^{(1)}$ with <i>t.i.</i>
$a_s M_1^{(0)}$	$\chi = 1.0$			$\chi = 2.0$		
0.00	1.297	0.485	0.485	0.833	0.620	0.620
0.01	-2.077	-2.889	-2.930	-2.539	-2.751	-2.793
0.05	-0.960	-1.772	-1.931	-1.419	-1.632	-1.794
0.10	-0.433	-1.246	-1.518	-0.895	-1.108	-1.379
0.50	0.975	0.163	-0.593	0.400	0.187	-0.465
1.00	1.658	0.845	-0.111	0.908	0.696	-0.058
2.00	2.274	1.461	0.434	1.332	1.119	0.363
5.00	2.635	1.823	0.804	1.748	1.535	0.822
$a_s M_1^{(0)}$	$\chi = 3.0$			$\chi = 3.6$		
0.00	0.763	0.670	0.670	0.747	0.683	0.683
0.01	-2.608	-2.701	-2.742	-2.624	-2.688	-2.728
0.05	-1.489	-1.581	-1.745	-1.505	-1.568	-1.732
0.10	-0.966	-1.059	-1.332	-0.982	-1.045	-1.319
0.50	0.301	0.208	-0.426	0.279	0.215	-0.415
1.00	0.757	0.665	-0.037	0.722	0.658	-0.029
2.00	1.092	0.999	0.348	1.029	0.966	0.346
5.00	1.408	1.316	0.770	1.301	1.237	0.750
$a_s M_1^{(0)}$	$\chi = 4.0$			$\chi = 5.0$		
0.00	0.740	0.689	0.689	0.729	0.697	0.697
0.01	-2.631	-2.682	-2.722	-2.642	-2.674	-2.713
0.05	-1.511	-1.562	-1.726	-1.522	-1.554	-1.718
0.10	-0.988	-1.040	-1.313	-0.999	-1.031	-1.305
0.50	0.269	0.217	-0.410	0.255	0.222	-0.403
1.00	0.706	0.655	-0.026	0.684	0.651	-0.021
2.00	1.002	0.951	0.345	0.960	0.928	0.345
5.00	1.249	1.198	0.740	1.165	1.133	0.724
$a_s M_1^{(0)}$	$\chi = 5.3$			$\chi = 6.0$		
0.00	0.727	0.698	0.698	0.723	0.701	0.701
0.01	-2.644	-2.673	-2.712	-2.648	-2.670	-2.709
0.05	-1.524	-1.553	-1.716	-1.528	-1.550	-1.714
0.10	-1.001	-1.030	-1.303	-1.005	-1.027	-1.301
0.50	0.252	0.223	-0.401	0.247	0.225	-0.398
1.00	0.679	0.650	-0.020	0.672	0.649	-0.017
2.00	0.952	0.923	0.344	0.937	0.915	0.345
5.00	1.148	1.119	0.720	1.116	1.093	0.714

TABLE X. One-loop wave function renormalization for action \mathcal{S}^B in Landau gauge. Numerical integration errors are as in Table IX.

Action \mathcal{S}^D $\alpha_g = 1.0$						
$a_s M_1^{(0)}$	$Z_{2,dp_0}^{(1)}$ no <i>t.i.</i>	$Z_{2,dp_0}^{(1)}$ with <i>t.i.</i>	$Z_2^{(1)}$ with <i>t.i.</i>	$Z_{2,dp_0}^{(1)}$ no <i>t.i.</i>	$Z_{2,dp_0}^{(1)}$ with <i>t.i.</i>	$Z_2^{(1)}$ with <i>t.i.</i>
	$\chi = 1.0$			$\chi = 2.0$		
0.00	0.619	-0.194	-0.194	0.102	-0.111	-0.111
0.01	-2.755	-3.568	-3.597	-3.270	-3.482	-3.511
0.05	-1.636	-2.448	-2.601	-2.146	-2.358	-2.510
0.10	-1.107	-1.920	-2.185	-1.617	-1.830	-2.088
0.50	0.320	-0.493	-1.262	-0.287	-0.500	-1.146
1.00	1.034	0.221	-0.781	0.258	0.045	-0.728
2.00	1.710	0.898	-0.178	0.735	0.523	-0.272
5.00	2.138	1.325	0.304	1.217	1.005	0.274
	$\chi = 3.0$			$\chi = 3.6$		
0.00	0.038	-0.054	-0.054	0.027	-0.036	-0.036
0.01	-3.332	-3.425	-3.454	-3.344	-3.407	-3.436
0.05	-2.209	-2.302	-2.452	-2.221	-2.284	-2.435
0.10	-1.682	-1.775	-2.033	-1.694	-1.757	-2.015
0.50	-0.383	-0.476	-1.098	-0.403	-0.467	-1.082
1.00	0.112	0.019	-0.692	0.078	0.015	-0.679
2.00	0.499	0.406	-0.274	0.438	0.375	-0.271
5.00	0.878	0.786	0.220	0.770	0.707	0.200
	$\chi = 4.0$			$\chi = 5.0$		
0.00	0.023	-0.028	-0.028	0.016	-0.016	-0.016
0.01	-3.348	-3.399	-3.428	-3.354	-3.387	-3.415
0.05	-2.225	-2.276	-2.426	-2.231	-2.264	-2.414
0.10	-1.698	-1.749	-2.007	-1.705	-1.737	-1.995
0.50	-0.412	-0.463	-1.075	-0.424	-0.456	-1.063
1.00	0.064	0.013	-0.674	0.043	0.011	-0.663
2.00	0.412	0.361	-0.269	0.372	0.340	-0.265
5.00	0.720	0.668	0.191	0.635	0.603	0.176
	$\chi = 5.3$			$\chi = 6.0$		
0.00	0.015	-0.014	-0.014	0.013	-0.009	-0.009
0.01	-3.355	-3.384	-3.413	-3.358	-3.380	-3.409
0.05	-2.233	-2.261	-2.411	-2.235	-2.257	-2.407
0.10	-1.706	-1.735	-1.992	-1.709	-1.731	-1.988
0.50	-0.426	-0.455	-1.061	-0.430	-0.452	-1.057
1.00	0.039	0.010	-0.661	0.031	0.009	-0.658
2.00	0.364	0.335	-0.264	0.350	0.328	-0.262
5.00	0.618	0.589	0.173	0.586	0.563	0.168

TABLE XI. One-loop wave function renormalization for action \mathcal{S}^D in Feynman gauge. Numerical integration errors are as in Table IX.

Action \mathcal{S}^D $\alpha_g = 0.0$						
	$Z_{2,dp_0}^{(1)}$ no <i>t.i.</i>	$Z_{2,dp_0}^{(1)}$ with <i>t.i.</i>	$Z_2^{(1)}$ with <i>t.i.</i>	$Z_{2,dp_0}^{(1)}$ no <i>t.i.</i>	$Z_{2,dp_0}^{(1)}$ with <i>t.i.</i>	$Z_2^{(1)}$ with <i>t.i.</i>
$a_s M_1^{(0)}$	$\chi = 1.0$			$\chi = 2.0$		
0.00	1.127	0.314	0.314	0.612	0.399	0.399
0.01	-2.246	-3.058	-3.097	-2.758	-2.971	-3.007
0.05	-1.127	-1.939	-2.095	-1.635	-1.847	-2.003
0.10	-0.598	-1.410	-1.679	-1.106	-1.319	-1.580
0.50	0.828	0.016	-0.756	0.223	0.011	-0.637
1.00	1.542	0.730	-0.274	0.768	0.555	-0.219
2.00	2.219	1.407	0.330	1.246	1.033	0.238
5.00	2.646	1.834	0.811	1.727	1.514	0.784
$a_s M_1^{(0)}$	$\chi = 3.0$			$\chi = 3.6$		
0.00	0.537	0.444	0.444	0.521	0.457	0.457
0.01	-2.833	-2.926	-2.960	-2.849	-2.913	-2.947
0.05	-1.710	-1.803	-1.959	-1.727	-1.790	-1.946
0.10	-1.183	-1.276	-1.537	-1.200	-1.263	-1.524
0.50	0.116	0.023	-0.600	0.091	0.027	-0.590
1.00	0.610	0.518	-0.194	0.572	0.509	-0.186
2.00	0.996	0.904	0.224	0.932	0.868	0.222
5.00	1.376	1.283	0.717	1.263	1.200	0.693
$a_s M_1^{(0)}$	$\chi = 4.0$			$\chi = 5.0$		
0.00	0.514	0.463	0.463	0.504	0.471	0.471
0.01	-2.856	-2.907	-2.941	-2.867	-2.899	-2.932
0.05	-1.733	-1.785	-1.940	-1.744	-1.776	-1.932
0.10	-1.207	-1.258	-1.519	-1.217	-1.250	-1.510
0.50	0.080	0.029	-0.585	0.064	0.031	-0.578
1.00	0.556	0.505	-0.182	0.531	0.499	-0.176
2.00	0.903	0.852	0.222	0.859	0.827	0.223
5.00	1.210	1.159	0.682	1.122	1.090	0.663
$a_s M_1^{(0)}$	$\chi = 5.3$			$\chi = 6.0$		
0.00	0.502	0.473	0.473	0.498	0.476	0.476
0.01	-2.868	-2.897	-2.929	-2.872	-2.895	-2.926
0.05	-1.746	-1.775	-1.930	-1.749	-1.772	-1.927
0.10	-1.219	-1.248	-1.509	-1.223	-1.246	-1.506
0.50	0.061	0.032	-0.576	0.055	0.033	-0.573
1.00	0.526	0.497	-0.175	0.517	0.495	-0.173
2.00	0.851	0.822	0.223	0.835	0.813	0.224
5.00	1.104	1.075	0.660	1.071	1.049	0.654

TABLE XII. One-loop wave function renormalization for action \mathcal{S}^D in Landau gauge. Numerical integration errors are as in Table IX.

Action \mathcal{S}^B $\chi = 4.0$				
$a_s M_1^{(0)}$	regular	tadpole	$C_0^{(1)}$ no t.i. (reg + tad)	$C_0^{(1)}$ with t.i.
	$\alpha_g = 1.0$			
0.00	-0.618(3)	1.474	0.856(3)	-0.343(3)
0.01	-0.616(8)	1.474	0.858(8)	-0.341(8)
0.05	-0.617(5)	1.474	0.857(5)	-0.342(5)
0.10	-0.617(5)	1.474	0.857(5)	-0.342(5)
0.50	-0.608(3)	1.474	0.866(3)	-0.333(3)
1.00	-0.587(2)	1.474	0.887(2)	-0.312(2)
2.00	-0.547(2)	1.474	0.927(2)	-0.272(2)
5.00	-0.519(2)	1.474	0.955(2)	-0.244(2)
10.00	-0.561(2)	1.474	0.913(2)	-0.286(2)
	$\alpha_g = 0.0$			
0.00	-0.345(3)	1.199	0.854(3)	-0.345(3)
0.01	-0.351(8)	1.199	0.848(8)	-0.351(8)
0.05	-0.347(5)	1.199	0.852(5)	-0.347(5)
0.10	-0.347(5)	1.199	0.852(5)	-0.347(5)
0.50	-0.333(3)	1.199	0.866(3)	-0.333(3)
1.00	-0.312(2)	1.199	0.887(2)	-0.312(2)
2.00	-0.273(2)	1.199	0.926(2)	-0.273(2)
5.00	-0.244(2)	1.199	0.955(2)	-0.244(2)
10.00	-0.286(2)	1.199	0.913(2)	-0.286(2)

TABLE XIII. One-loop speed of light renormalization for action \mathcal{S}^B for different $a_s M_1^{(0)}$ values at fixed anisotropy $\chi = 4.0$. Where errors are not indicated explicitly, they are of $O(1)$ or less in the last digit.

Action \mathcal{S}^B				
	$C_0^{(1)}$ <i>no t.i.</i>	$C_0^{(1)}$ <i>with t.i.</i>	$C_0^{(1)}$ <i>no t.i.</i>	$C_0^{(1)}$ <i>with t.i.</i>
$a_s M_1^{(0)}$	$\chi = 1.0$		$\chi = 2.0$	
0.00	-0.039	-0.019	0.668	-0.210
0.01	-0.036	-0.015	0.671	-0.207
0.05	-0.038	-0.018	0.669	-0.208
0.10	-0.044	-0.023	0.669	-0.209
0.50	-0.127	-0.107	0.654	-0.223
1.00	-0.265	-0.245	0.633	-0.244
2.00	-0.509	-0.488	0.582	-0.295
5.00	-0.749	-0.728	0.432	-0.446
$a_s M_1^{(0)}$	$\chi = 3.0$		$\chi = 3.6$	
0.00	0.807	-0.302	0.842	-0.330
0.01	0.809	-0.300	0.843	-0.328
0.05	0.808	-0.301	0.842	-0.329
0.10	0.807	-0.302	0.842	-0.330
0.50	0.811	-0.298	0.849	-0.322
1.00	0.821	-0.288	0.867	-0.304
2.00	0.836	-0.273	0.899	-0.272
5.00	0.802	-0.307	0.907	-0.264
$a_s M_1^{(0)}$	$\chi = 4.0$		$\chi = 5.0$	
0.00	0.856	-0.343	0.880	-0.363
0.01	0.858	-0.341	0.882	-0.361
0.05	0.857	-0.342	0.881	-0.362
0.10	0.857	-0.342	0.881	-0.362
0.50	0.866	-0.333	0.893	-0.350
1.00	0.887	-0.312	0.918	-0.325
2.00	0.927	-0.272	0.969	-0.274
5.00	0.955	-0.244	1.031	-0.212
$a_s M_1^{(0)}$	$\chi = 5.3$		$\chi = 6.0$	
0.00	0.885	-0.367	0.893	-0.374
0.01	0.887	-0.365	0.896	-0.372
0.05	0.886	-0.366	0.895	-0.373
0.10	0.886	-0.366	0.895	-0.373
0.50	0.898	-0.354	0.907	-0.360
1.00	0.924	-0.327	0.935	-0.332
2.00	0.977	-0.274	0.992	-0.275
5.00	1.046	-0.206	1.073	-0.194

TABLE XIV. One-loop speed of light renormalization for action \mathcal{S}^B . Numerical integration errors are at the ± 0.008 level for $a_s M_1^{(0)} = 0.01$, at the ± 0.005 level for $a_s M_1^{(0)} = 0.05$ and 0.10 and at the ± 0.003 level or less for other masses.

$a_s M_1^{(0)}$	Action \mathcal{S}^A		Action $\mathcal{S}^{A'}$	
	$C_0^{(1)}$ <i>no t.i.</i>	$C_0^{(1)}$ <i>with t.i.</i>	$C_0^{(1)}$ <i>no t.i.</i>	$C_0^{(1)}$ <i>with t.i.</i>
0.00	0.000	0.000	0.000	0.000
0.01	0.000	0.000	0.000	0.000
0.05	0.000	0.000	0.000	0.000
0.10	-0.007	-0.007	-0.007	-0.007
0.50	-0.102	-0.102	-0.098	-0.098
1.00	-0.258	-0.258	-0.243	-0.243
2.00	-0.536	-0.536	-0.490	-0.490
5.00	-0.809	-0.809	-0.730	-0.730

TABLE XV. One-loop speed of light renormalization for actions \mathcal{S}^A and $\mathcal{S}^{A'}$. Numerical integration errors are as in Table XIV.

Action \mathcal{S}^D				
	$C_0^{(1)}$ <i>no t.i.</i>	$C_0^{(1)}$ <i>with t.i.</i>	$C_0^{(1)}$ <i>no t.i.</i>	$C_0^{(1)}$ <i>with t.i.</i>
$a_s M_1^{(0)}$	$\chi = 1.0$		$\chi = 2.0$	
0.00	-0.424	-0.139	0.213	-0.301
0.01	-0.421	-0.137	0.216	-0.298
0.05	-0.424	-0.139	0.213	-0.301
0.10	-0.430	-0.146	0.211	-0.303
0.50	-0.525	-0.241	0.179	-0.335
1.00	-0.683	-0.398	0.129	-0.385
2.00	-0.971	-0.686	0.033	-0.482
5.00	-1.275	-0.991	-0.180	-0.694
$a_s M_1^{(0)}$	$\chi = 3.0$		$\chi = 3.6$	
0.00	0.320	-0.388	0.345	-0.415
0.01	0.324	-0.385	0.348	-0.412
0.05	0.321	-0.387	0.346	-0.414
0.10	0.319	-0.390	0.344	-0.415
0.50	0.305	-0.404	0.334	-0.426
1.00	0.286	-0.422	0.324	-0.436
2.00	0.256	-0.452	0.311	-0.448
5.00	0.167	-0.541	0.266	-0.494
$a_s M_1^{(0)}$	$\chi = 4.0$		$\chi = 5.0$	
0.00	0.356	-0.427	0.372	-0.446
0.01	0.358	-0.425	0.375	-0.443
0.05	0.356	-0.426	0.373	-0.444
0.10	0.355	-0.427	0.372	-0.446
0.50	0.347	-0.436	0.367	-0.451
1.00	0.340	-0.443	0.365	-0.453
2.00	0.335	-0.447	0.372	-0.446
5.00	0.311	-0.471	0.382	-0.436
$a_s M_1^{(0)}$	$\chi = 5.3$		$\chi = 6.0$	
0.00	0.375	-0.450	0.381	-0.457
0.01	0.378	-0.446	0.384	-0.453
0.05	0.376	-0.448	0.383	-0.455
0.10	0.376	-0.449	0.382	-0.455
0.50	0.371	-0.454	0.378	-0.459
1.00	0.370	-0.455	0.379	-0.459
2.00	0.379	-0.446	0.392	-0.446
5.00	0.396	-0.429	0.421	-0.416

TABLE XVI. One-loop speed of light renormalization for action \mathcal{S}^D . Numerical integration errors are as in Table XIV.

FIGURES

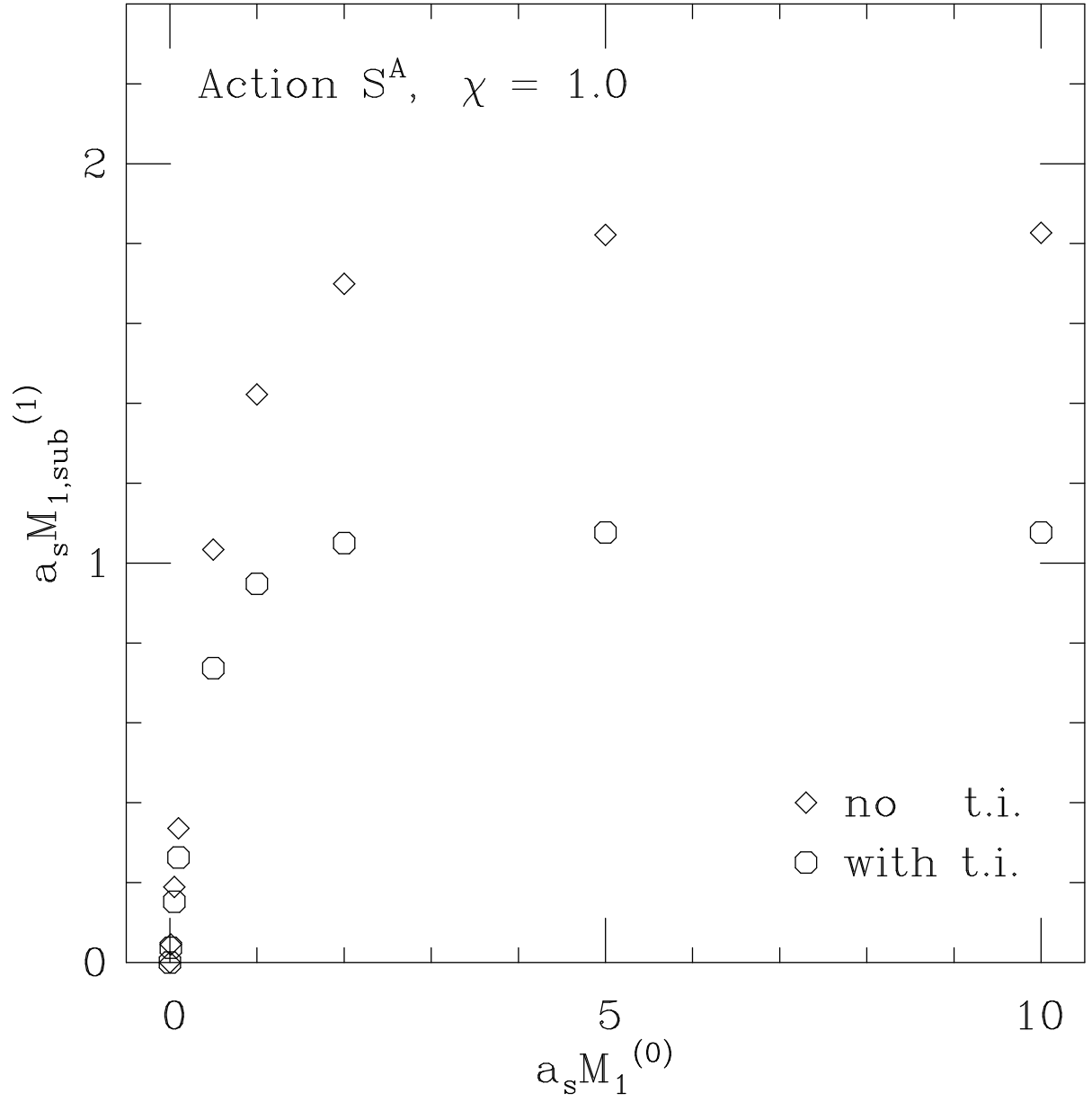


FIG. 1. $a_s M_{1,sub}^{(1)}$ versus $a_s M_1^{(0)}$ both with and without tadpole improvement for action S^A .

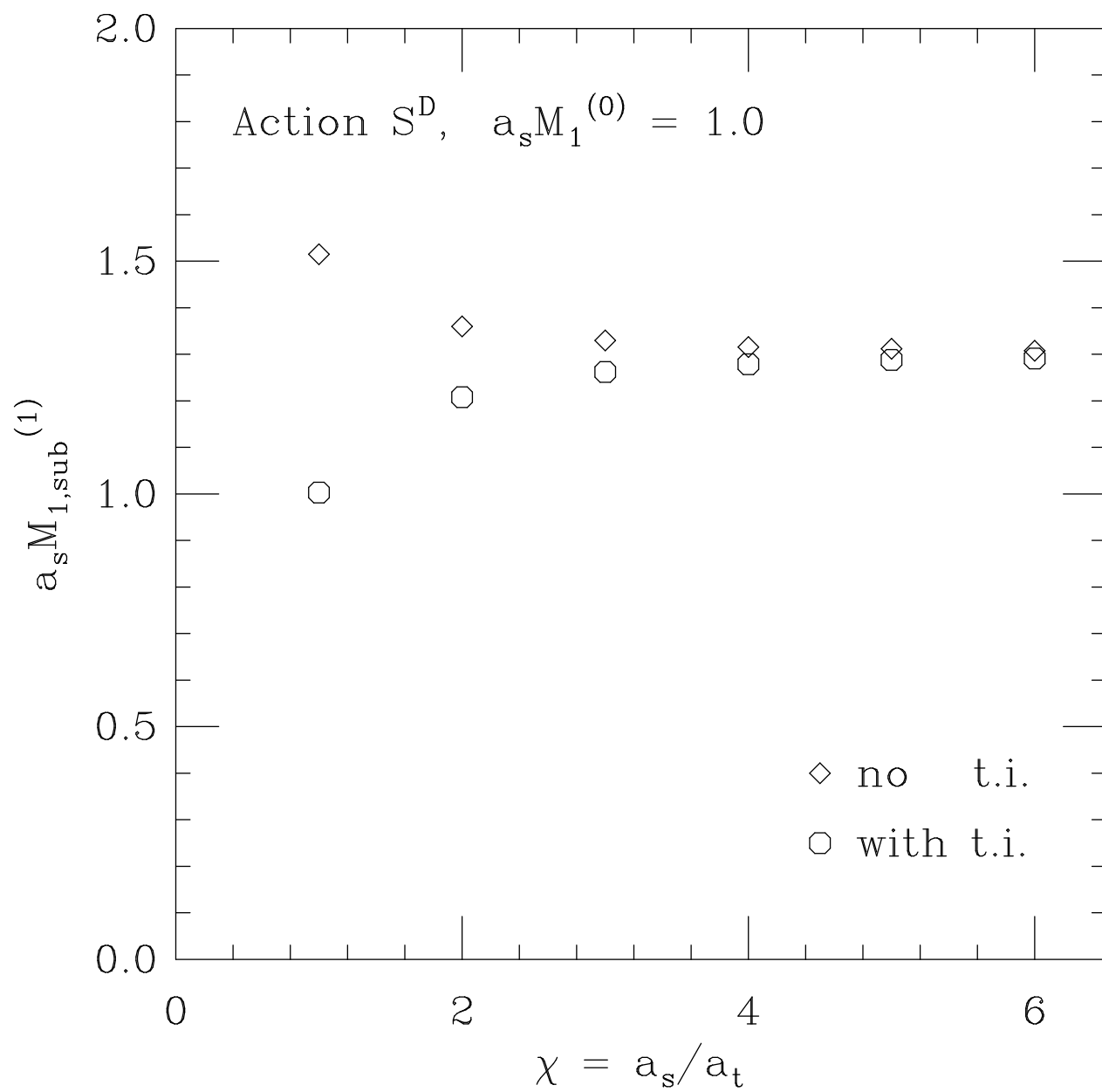


FIG. 2. $a_s M_{1,sub}^{(1)}$ versus χ both with and without tadpole improvement for action S^A .

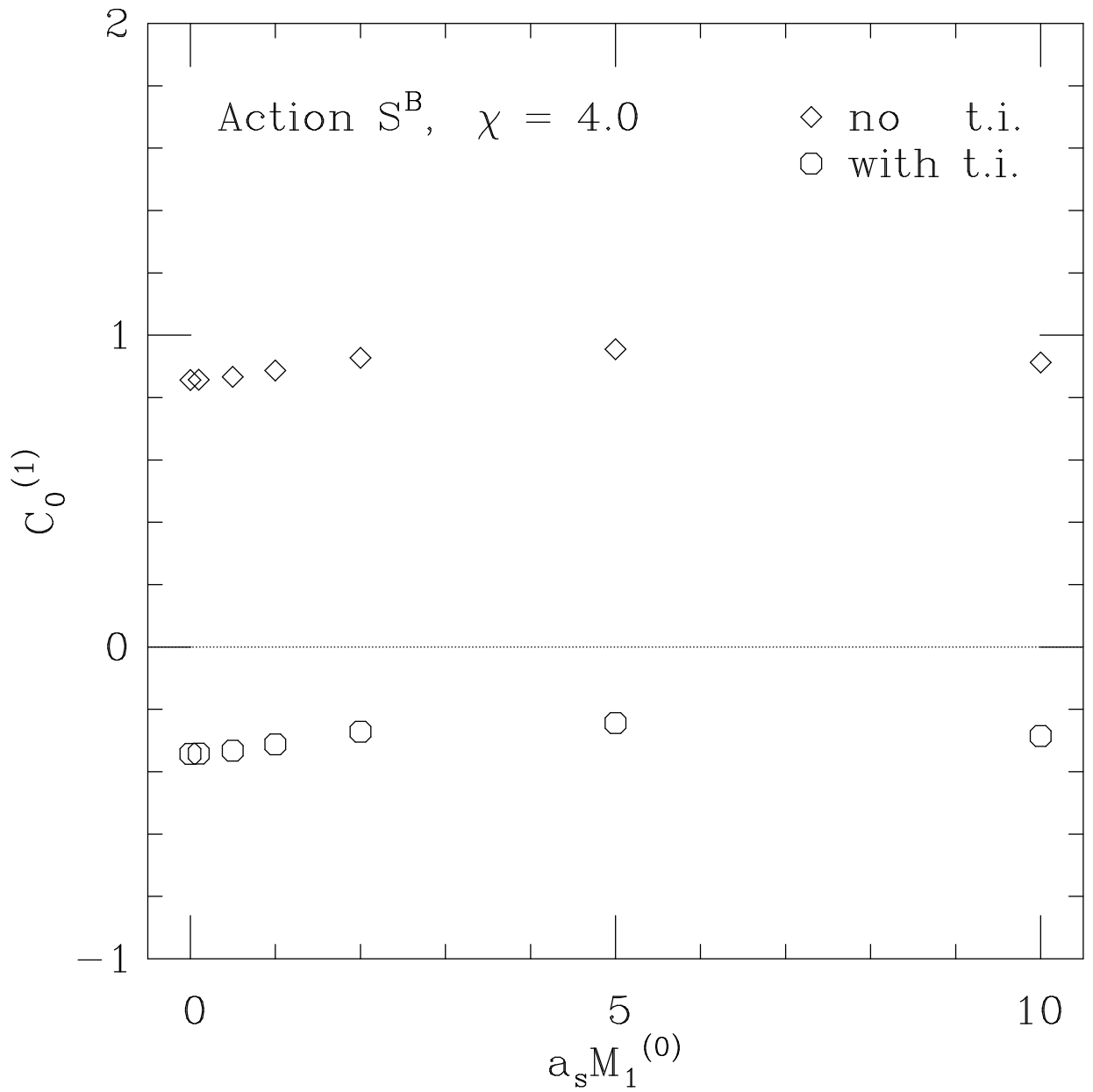


FIG. 3. $C_0^{(1)}$ versus $a_s M_1^{(0)}$ both with and without tadpole improvement for action S^B .

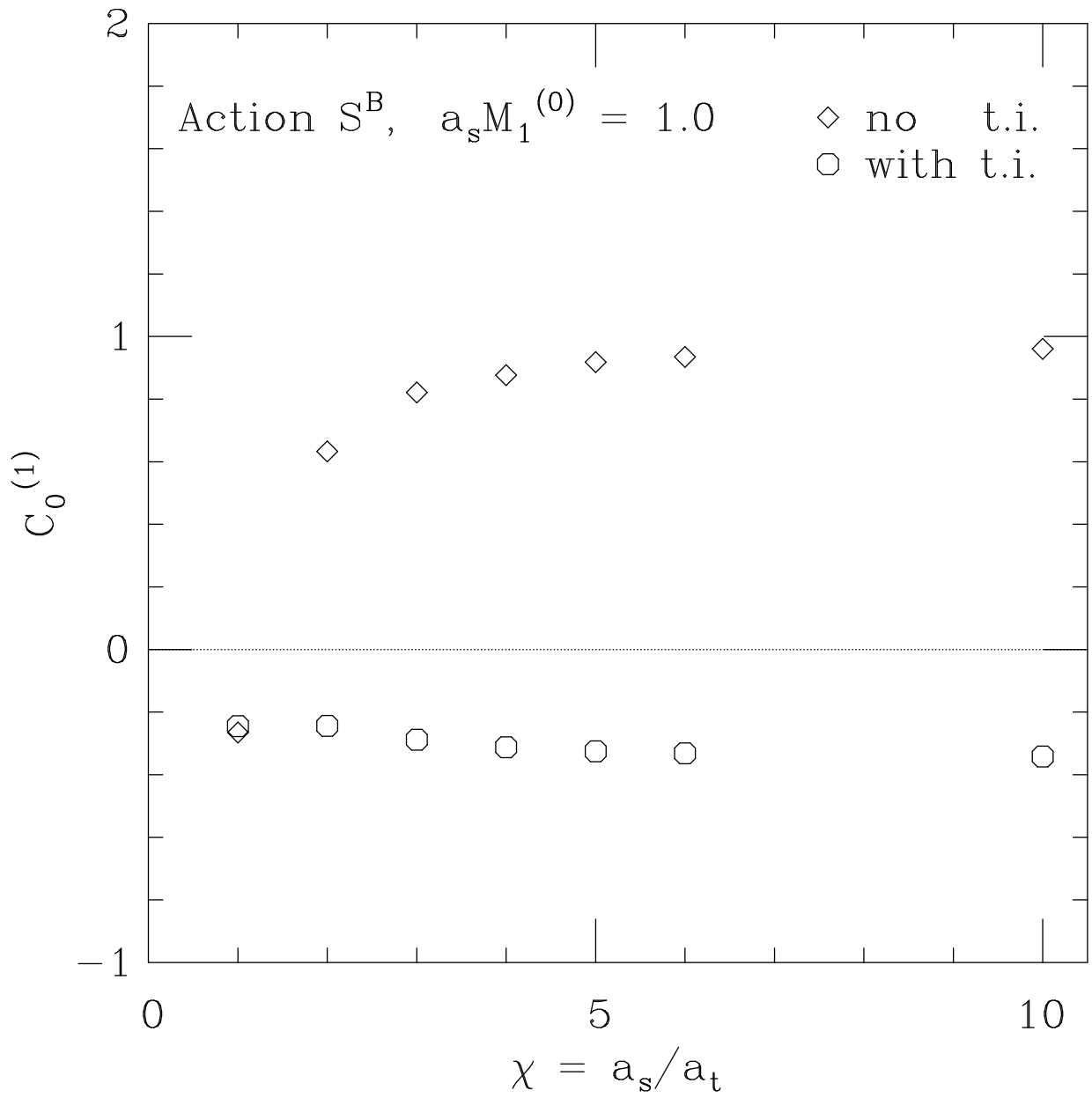


FIG. 4. $C_0^{(1)}$ versus χ both with and without tadpole improvement for action S^B .